Flow of Tangent hyperbolic nanofluid in Darcy-Forchheimer porous medium over a stretching cylinder with motile gyrotactic microorganism

Thesis Submitted By

ASMA JABEEN
(01-248182-001)

Supervised By

Prof. Dr. Muhammad. Ramzan

A dissertation submitted in fulfillment of the requirements for the award of the degree of MS (Mathematics)

Department of Computer Science
BAHRIA UNIVERSITY ISLAMABAD

SEPTEMBER 2020

Dedicated to

My Beloved Parents

and

Respected Supervisor

Acknowledgments

I am thankful to **ALLAH**Almighty, the most Gracious and the most merciful who bestowed me with His great blessings. I am really blessed as He gave me the ability to learn and to achieve my goal. He gave me a source (His beloved **Prophet (PBUH)**) of light and guidance for my way.

My acknowledgment is to my kind, passionate and diligent supervisor, Prof. Dr. M. Ramzan, who supported me with his great opinions and inspirational thoughts.My intense gratitude is to my honorable teachers. In particular, Dr. Jafar Hasnain and Dr. Rizwan-ul-haq who have always been supportive in all of my course work. I'm blessed to have them in my life...

My intense recognition is to my mother, father and my siblings who are always real pillars for my encouragement and showed their everlasting love, care and support throughout my life.

I would like to express my special thanks to my seniors and PhD students who were always remained helpful to me. May Allah shower His blessings upon them more than enough.

Asma Jabeen

Bahria University Islamabad, Pakistan

October, 06, 2020

Abstract

A mathematical model is investigated to scrutinize flow of Tangent hyperbolic Nanofluid in Darcy-Forchheimer porous medium over a stretching cylinder with convective heat and mass conditions.The heat and mass transfer phenomena are visualized in the presence of melting heat and gyrotactic microorganisms.Fluid is electrically conducted in the attendance of applied magnetic field. Appropriate transformations procedure is implemented for the transition of partial differential equations to ordinary one and then computer software-based MATLAB function bvp4c is implemented to handle the envisioned mathematical model. The deliberation of numerous parameters versus the velocity, heat and mass transfer and density of gyrotactic microorganisms are portrayed through graphs. It is witnessed that velocity of the fluid is decreased for increasing values of porosity number and the increasing value of melting heat reduces the temperature. Furthermore the microorganisms profile dwindles for increasing estimates of Peclet number. Local Nusselt number,Local Sherwood number and density number of motile microorganismsare evaluated via tables. An outstanding matching is obtained when the results obtained in the current analysis are compared with an established result in the literature.

Bahria University
Discovering Knowledge

Thesis Revision Certificate

Student's Name: **ASMA JABEEN** Registration No: **59044**

Program of Study: **MS Mathematics**

Thesis Title:

It is to certify that the above student's thesis document has been revised in the light of examiners suggestions and to my satisfaction and, to my belief, its standard is appropriate for acceptance.

Principal Supervisor's Signature:

Date: 26-11-2020

Name: Prof. Dr. Muhammad Ramzan

Bahria University

Discovering Knowledge

MS-13

Thesis Completion Certificate

Student's Name: **Asma Jabeen** Registration No**: 59044**

Program of Study: **MS(Mathematics)** Thesis Title: **"Flow of Tangent hyperbolic nanofluid in Darcy-Forchheimer porous medium over a stretching cylinder with motile gyrotactic microorganism"**

It is to certify that the above student's thesis has been completed to my satisfaction and, to my belief, its standard is appropriate for submission for Evaluation. I have also conducted plagiarism test of this thesis using HEC prescribed software and found similarity index at **01%** that is within the permissible limit set by the HEC for the MS/MPhil degree thesis. I have also found the thesis in a format recognized by the BU for the MS/MPhil thesis.

Principal Supervisor's Signature: _____

Date: 03-10-2020 **Name: Prof. Dr. Muhammad Ramzan**

Bahria University

Discovering Knowledge

MS-14A

Author's Declaration

I, **Asma Jabeen** hereby state that my MS thesis titled **"Flow of Tangent hyperbolic nanofluid in Darcy-Forchheimer porous medium over a stretching cylinder with motile gyrotactic microorganism"** is my own work and has not been submitted previously by me for taking any degree from this university **Bahria University Islamabad** or anywhere else in the country/world. At any time if my statement is found to be incorrect even after my Graduate the university has the right to withdraw/cancel my MS degree.

Name of scholar: **Asma Jabeen**

Registration no: **59044**

Bahria University

Discovering Knowledge

MS-14B

Plagiarism Undertaking

I solemnly declare that research work presented in the thesis titled **"Flow of Tangent hyperbolic nanofluid in Darcy-Forchheimer porous medium over a stretching cylinder with motile gyrotactic microorganism"** is solely my research work with no significant contribution from any other person. Small contribution / help wherever taken has been duly acknowledged and that complete thesis has been written by me.

I understand the zero tolerance policy of the HEC and Bahria University towards plagiarism. Therefore I as an Author of the above titled thesis declare that no portion of my thesis has been plagiarized and any material used as reference is properly referred / cited.

I undertake that if I am found guilty of any formal plagiarism in the above titled thesis even after award of MS degree, the university reserves the right to withdraw / revoke my MS degree and that HEC and the University has the right to publish my name on the HEC / University website on which names of students are placed who submitted plagiarized thesis.

Student / Author's Sign:_____

Name of the Student: **Asma Jabeen**

Contents

List of Tables

List of Figures

Nomenclature

Symbols

u,w	Axial and Radial velocity components
B_0	Magnetic field strength
T	Temperature
T_f	Heated fluid temperature
T_∞	Ambient fluid temperature
C	Concentration
C_f	Heated fluid Concentration
C_∞	Ambient fluid Concentration
U_0	Reference velocity
L	Characteristic length
K	Thermal conductivity
D_B	Brownian diffusion coefficient
D_T	Thermophoretic diffusion coefficient
H	Convective heat transfer coefficient
k_m	Wall mass transfer coefficient
A	Radius of cylinder
D_m	Molecular diffusivity of species concentration

Pr	Prandtl number
M	Hartman number
N_b	Brownian motion parameter
N_t	Thermophoresis parameter
Sc	Schmidt number
N_r	Buoyancy ratio
q_w	Surface heat flux
h_m	Surface mass flux
Nu_z	Local Nusselt number
Sh_z	Local Sherwood number
Re_z	Local Reynolds number
Nn_z	Density number of motile microorganisms
n^*	Power law index
Γ	Williamson parameter
n	Density of the motile microorganism
n_∞	Concentration of microorganisms
n_f	Constant motile microorganism
D_n	Diffusivity of the microorganism
C_s	Heat capacity

T_m	Melting temperature
T_0	Solid temperature
We	Local Weissenberg number
K^*	Porous medium permeability
F_1	Local Inertia coefficient of the porous medium
Lb	Bioconvection Lewis number
Pe	Peclet number
Pr	Prandtl number
W_c	Constant maximum cell swimming speed
k_1	Permeability of porous medium
C_b	Drag coefficient
q_n	Surface motile microorganism flux
σ	Electrical conductivity (s3 A2 kg1 m3)
ν	Kinematic viscosity
ρ	Density
γ	Curvature parameter
γ^*	Average volume of microorganism
ρ_m	Density of microorganism
N_c	Rayleigh number

λ^*	Latent heat of fluid
λ	Mixed convection parameter
ν	Viscosity
ϕ	Dimensionless fluid concentration
θ	Dimensionless temperature
H	Transformed coordinate
M_1	Melting number
α	Thermal diffusivity
τ	Ratio between heat capacity
β	Casson fluid parameter
β_T	Coefficient of thermal expansion
γ_1	Thermal Biot number
γ_2	Concentration Biot number
h_f, h_θ, h_ϕ	Non-zero auxiliary parameters
L_f, L_θ, L_ϕ	Linear operators
f_0, θ_0, ϕ_0	Initial approximations
$c_1, c_2 .. c_7$	Constants

Chapter 1

Introduction and Literature review

1.1 Introduction

The study of non-Newtonian liquids is an important subject, which is relevent to scientific investigation since last few decays. All of those fluid for which the shear rate is changed and the shear stress stay unaltered are consider to be non-Newtonian liquids. Then non-Newtonian liquids does not show the linear relation along velocity gradient and shear stress. Newton's law of viscosity does not followed by non-Newtonian liquids. It has been categorized into three types: rate, integration and differential type. And it has vital applications in technology, engineering and industrial process, like as plastic sheet formation, paper production, petroleum driling, biological solutions, ketchup and so forth. Casson fluid is a non-Newtonian fluid, which have infinite viscosity at zero rate of shear, and zero viscosity at an infinite rate of shear. Particularly, the model of Casson liquid tell us the accurate flow of blood at lowest shear rate when it flows from small arteries.

Nanofluid is an effective heat transfer fluid containing a mixture of nanoparticles (Fe, Cu, 1-100nm in size) and Base-fluid (water, Ethylene glycol, oil). Many fluids have thermal conductivities well below that of metals, limiting their ability to move large amounts of heat quickly. Most processes get around these limitations by increasing the

size of the heat exchangers. However, when other constraints limit physical sizes, the thermal conductivity (and even heat capacity) of the fluid may need to be changed. One method of accomplishing this is putting significant quantities of microscopic bits of metals into the fluid. As long as these particles remain in suspension, you gain some of the thermal benefits of fluid while still retaining the fluidity of the base fluid. Nanofluid is the colloidal suspension of nano sized particles in any base fluid. The thermal conductivity of most of the solids are higher than any base heat transfer fluids(water,engine oil,ethylene glycol etc). Because,while preparing nano fluid, we are mixing nano sized solid particles of higher thermal conductivity to normal base fluid, the thermal conductivity of the nanofluid increases. But in contrast, if the thermal conductivty of solid particle that is mixed is lesser than that of base fluid,the thermal conductivity of nanofluid decreases. As the temperature increases, the intermolecular attraction between the nanoparticles and their base fluids weakens. Hence, the viscosity of nanofluids decreases with the increase in temperature. Nanoparticles are not self propelled their movement is driven by Brownian motion. The nanoparticles having irregular movement in the nanofluid with diameter not more than 100nm is called Brownian motion. Nanofluid have applications in electronic cooling, transportation, surface coating, biochemical and engine oils etc. There are four following properties of nanofluid.

· Nonlinear development in thermal-conductivity using nanoparticles.

· Enhancement of thermal conducitivity using low concentration of nanoparticles.

· Augmentation in boiling crucial heat flux.

· Potent temperature dependent thermal-conductivity.

Henry Darcy first defined the idea of liquid passes through a porous media in 1856. Darcy Forchheimer effect is the modification of Darcian flow having inertia term with boundary conditions. Forchheimer term is introduced by Muskat in 1946. Darcy law is any term or calculations that illustrate the flow of fluid across a spongy surface and is valid for viscous and high flow rate. Any flow having Reynolds number not more than one is apparently laminar then Darcy law will be applied on it. In melting process, thermal

energy is put away in a material through latent heat.

The model of Tangent hyperbolic liquid is an important class of non-Newtonian fluid model. The term Tangent hyperbolic nanoliquid corresponds to the mixture of non-Newtonian Tangent hyperbolic fluid and nano-size particles. The density of gyrotactic microorganisms is might be denser than water so they swim upward in a fluid with free stress and having rigid boundary on the steadiness of the suspension in a fluid, this process is known as "Biconvection". Gyrotax is self propelled and increases the suspension of nanofluid.

1.2 Literature Review

The term Nano-fluid was first examined by Choi [1], to explain the fluid suspension, due to ultrafine of nanoparticles it has unique chemical and physical properties [2]. Nanoparticles are basic forming components of nanofluid. Nanoparticles have higher surface area to volume ratio and have large thermal conductivity as compared to micro-sized particles, they occupy large number of atoms on boundaries which gives them high stability in suspensions, and can help in future with coefficient thermal management systems and designing. Nanofluids with a wide particle distribution have better packing ability than those of narrow particle distribution keeping constant volume fraction. This suggests that a wide distribution of nanoparticle provides more free space to move around and eventually makes the sample less viscous. It has been found that there is exceptional rise in viscosity with a rise in volume concentration. Nanoparticle inclusion even at a low volume fraction in the host liquid increased the nanoparticle concentration and greatly increased the viscosity. Infact, with the addition of more particles, the effect of viscosity turns out to be detrimental to the heat transfer system. The applications of nano liquid on nuclear reactor is explained by Boungiorno et al. [3]. Nano-fluids are most beneficial then their base fluids, more economical and used for the safety of nuclear reactor. Nano-liquid with extraordinary heat transit property is the most discoursed subject of present

time [4 − 5]. Pop and Khan [6] explained the boundary layer flow of nano liquids through a stretch surface, they initiated that thermophoresis effect and Brownian motion are important. Nield and Kuznetsov [7] explained the convective flow of nanoliquid through a vertically flat surface. Ferdows et al. [8] investigated the unsteady flow of viscous nano liquid over a spongy media. The combination of forced and natural convection flow is initiated as mixed convection and it arise in industrially and natural processes. The variation in concentration and temperature causes buoyancy forces in mixed convection flow. Nazar et al. [9] discussed the mixed convection flow of liquid with porous media saturated by a nanoliquids over a circular cylinder. Its noted that by heating cylinder, the boundary layer separation delays and by cooling cylinder, its boundary layer separation comes near to the lower point of stagnation. Pressure is generated due to the buoyancy forces at the boundary layer of liquid, which causes an increment in the concentration and temperature of the liquid.

Mixed convection flow of convective nanoliquids flow through a stretching cylinder is examined by Dinarvand et al. [10]. Mixed convection flow have numerous applications in technology and industry in nature. For example; exposed to wind current, solar reciever, electronic devices cooled by fans, flows in the atmosphere and in the ocean etc. Concentration and temperature differences give rise to buoyancy forces in mixed convection. Fluid flows through a porous media have significance in industrial, chemical, environmental and pharmaceutical system. It also use in ground water system, energy storage units, geothermal heat exchanger layout, nuclear waste disposal, crude oil production and water movement in reservoirs. The liquid flowing through a stretch cylinder have numerous applications in engineering process. For example, glass fiber, by manufacturing of food, paper production, drawing of films and plastic wire, liquid films in condensational process, and crystal growing.

Forchheimer [11] described the squared velocity gradient in the equation of motion. The term Forchheimer is named by Muskat [12]. Convective flow of saturated porous media with thermophoresis feature and viscous dissipation is examined by Seddeek [13].

The Darcy-Forchheimer Brinkman relation through convective nanofluid is examined by Umavathi et al. [14]. Henry Darcy [15] described the liquid flow through a spongy surface, which based on the result of experiment on the flow of water over cribs of sand on hydrogeology in the earth sciences. For the water flow he studied the aspects of sand filters. After his experiment he deliberated that viscous forces dominate around inertia forces with in porous media. Afterwards which becomes Darcy-law. Darcy law presumes laminar flow of the fluid in the absence of density/inertia term which indicates that absence of inertia term is not the case in classical Navier-stokes equations. Alzahrani [16] describe the significance of Darcy-Forchheimer porous media in nanoliquids through a stretching surface. The flow of Casson liquid with rotation parameter on the primary velocity gradient with Darcy-Forchheimer effect is examined by Mandal and Seth [17]. They noted that primary velocity is closest to the stretching surface and reversed to the secondary velocity.

Nourazar et al. [18] described the MHD thermal flow of nanoliquid pass through a spongy surface over a stretching cylinder. Recently, many researcher and scientist gained so much attentions towards the MHD nanoliquids flow through a porous media beacause of innumerable applications in industry and engineering. MHD flow of nano liquids by convected heat through a stretching surface is studied by Hayat et al. [19]. The flow of liquid at boundary layer and heat transfer have crucial applications in engineering and industry. Applications related to energy transfer are for astrophysical flows, reboiler, plasma, electrical heating jacket, steam jacketing or coil, and nuclear reactors cooling. Heat transfer in magnetohydrodynamics (MHD) fraction inertia flow is studied by Rasheed and Anwar [20]. Magnetohydrodynamics (MHD) flow through stretched cylinder with heterogenous-homogeneous reactions and Newtonian heat is investigated by Hayat et al. [21]. MHD flow of an electrically conducting flow have numerous applications in metallurgical metal-working processes, engineering process like as MHD generator, nuclear reactors, study of plasma, and extractional geothermal energy. MHD techniques used to purify the molten metals from non-metallic inclusion. Properties of

heat transfer in the flow of nanoliquid is discussed by Ganvir et al. [22].

Bioconvection is a process when convection is caused by upward direction of swimming motile gyrotactic microorganisms like algae. By adding microorganisms to a nanoliquid it increases the stability and mass transfer of a liquid as a suspension $[23-24]$. Because, upswimming of gyrotax, tend to concentration on the upper portion of the liquid cause a heavy density stratification that's mostly unstable $[25-26]$. Like gyrotax, another specie oxytactic microorganisms also causes biothermal convection [27]. The model of both gyrotax and oxytactic microorganisms is examined by Pedley and Hill [28]. The motion of nanoparticles is driven by thermophoresis and Brownian motion, and they are not self propelled, where as the motion of microorganisms are self propelled. Hence the motion of gyrotax does not depent upon the motion of nanoparticles [29]. Mutuku et al. [30] ,Pop and Xu et al. [31], Zaimi et al. [32], Tham et al. [33], Khan et al. [34], and many others scientist drawn an attention on the several research of both gyrotactic microorganisms and nanoliquid having nanoparticles.

The study of motion of electrically conducted liquid in the presence of magnetic field is identified as MHD. The effect of melting heat transfer process on the MHD flow of a Tangent Hyperbolic liquid is discussed by Hayat et al. [35]. By the process of melting heat thermal energy is store in a material by latent heat [36]. The Non-Newtonian melting heat transfer have crucial application in innovative thermal engineering, like as in latent heat, welding process, magma solidification, thermal protection melting of the permafrost, thermal insulation geothermal optimal utilization of energy, and in the development of semiconductor. Robert [37] discussed the process of melting heat of ice placed in a hoted air stream in the effect of steady state(t=0). The flow of laminar fluid pass through a static flate plate on the surface of melting heat transfer is studied by Cho [38] and Epstein [39]. Robert [40] discussed the phenomenon of melting heat in the steady state. Recently, non-Newtonian fluids having melting heat transfer have innumerable applications in innovational thermal engineering, as in latent heat thermal energy storage, welding processes, thermal insulation, magma solidification, optimal utilization of energy,

preparation of semiconductors, geothermal energy recovery, etc. Hayat et al. [41 − 42] examined the transfer of melting heat in the viscoelastic liquid flowing through a stretched cylinder and the effect of heterogeneous/homogeneous reactions. The transfer of melting heat has abundent significance in composition of frozen ground defrosting, laser fabrication magma solidification and storage of thermal energy. The behavior of heterogeneous/homogeneous reactions and the transfer of melting heat in the visco-elastic liquid flow through a stretch cylinder is described by Hayat et al. [43].

Chapter 2

Basic preliminaries and laws

This chapter contains some elementary defination, concepts and laws that are helpful in understanding work in the subsequent chapters.

2.1 Fluid

A substance that consist of particles and that particles constantly distorts when shear stress is applied. For example oil, paint, blood, ketchup, milk, and water etc.

2.1.1 Fluid mechanics

It is the class of natural science that deals with the behavior of fluids. It is futher classified into two classes.

2.1.2 Fluid statics

It is a class of fluid mechanics which explores the aspects of fluid properties at stationary state.

2.1.3 Fluid dynamics

It is a class of fluid mechanics which explores the aspects of fluid properties at motion.

2.2 Stress

Within the deformable body, the force per unit area is identied as stress. In SI its unit is (Nm^{-2}) and dimension is $\left[\frac{M}{LT^{-2}}\right]$. Mathematically,

$$\tau_{ji} = \frac{F_i}{A_j}, \qquad i, j = x, r \tag{2.1}$$

Here F_i and A_j are the componants of force and area respectively. It is further catogrized into two types.

2.2.1 Shear stress

The force that act on a substance parallel to the unit area of the surface is identified as shear stress.

2.2.2 Normal stress

The force that act on a substance perpendicular to the unit area of the surface is identified as normal stress.

2.3 Flow

Flow is specified as a material that continually deforms fluently under the effects of distinct form of forces. Flow is further categorised into two classes.

2.3.1 Laminar flow

Laminar flow is the phenomenon in flow field where fluid have uniform state and velocity is remain same at each measure.

2.3.2 Turbulent flow

A flow in which liquid flows irregularly and velocity changes at each measure is identified as turbulent flow.

2.4 Viscosity

The viscosity is an intensive property of liquid which estimates the internal resistance of liquid flow over deformation when numerous forces are acting on the fluid. It describes the behavior and motion of the fluid nearest the boundary. It is further divided into two types

2.4.1 Dynamic viscosity (μ)

It is to measure the resistivity of a liquid flow with an applied external force. Mathematically,

$$\mu = \frac{\text{Shear stress}}{\text{Gradient of velocity}}, \tag{2.2}$$

or

$$\mu = \frac{\tau_{yx}}{(du/dy)}. \tag{2.3}$$

Its SI unit is $\frac{ki\log ram}{meter.\sec}$ with dimension $\left[\frac{M}{LT}\right]$.

2.4.2 Kinematic viscosity (ν)

Kinematic viscosity is the ratio of the dynamic viscosity μ to the mass density ρ. The kinematic viscosity can be obtained by dividing the absolute viscosity of a fluid with the

fluid mass density. It is denoted by the Greek letter ν. Mathematically, we can write.

$$\nu = \frac{\text{Dynamic viscosity}}{\text{Fluid density}} = \frac{\mu}{\rho}, \tag{2.4}$$

Its SI unit is $\left(\frac{meter^2}{\text{sec}}\right)$ with dimension $\left[\frac{L^2}{T}\right]$.

2.4.3 Newton's law of viscosity

The liquids which demonstrate the direct and linear relationship between the gradient of velocity and shear stress. Mathematical expression of Newton's law of viscosity is:

$$\tau_{yx} \propto (du/dy), \tag{2.5}$$

or

$$\tau_{yx} = (\mu)(du/dy). \tag{2.6}$$

2.4.4 Viscous fluid

A fluid is identified as viscous fluid when offers resistance to flow. For example honey, petrol, glues, ketchup.

2.4.5 Newtonian fluid

Newtonian fluid is a satisfaction of Newton's law of viscosity and show the direct and linear correspondance between the shear stress and gradient of velocity. Here shear force τ_{yx} is linear correspondance to the gradient of velocity du/dy and μ is constant. For example, water, glycerin, benzene, ethyl alcohol, hexane etc.

2.5 Non-Newtonian fluids

Non-Newtonian liquid does not satisfies the Newton's law of viscosity and the relation between shear force τ_{yx} and gradient of velocity du/dy is not linear. For example honey, ketchup, toothpaste, blood, shampoo etc. Mathematical expression of Non-Newtonian fluid is.

$$\tau_{yx} \propto \left(\frac{du}{dy}\right)^n, n \neq 1, \tag{2.7}$$

or

$$\tau_{yx} = (K)\left(\frac{du}{dy}\right)^n, \tag{2.8}$$

This expression can be changed into Newton's law of viscosity when $K = \mu$ and $N = 1$, i.e.,

$$\tau_{yx} = (\mu)\left(\frac{du}{dy}\right), \qquad \mu = (K)\left(\frac{du}{dy}\right)^{n-1}. \tag{2.9}$$

2.6 Density

Density equals the mass per unit volume of a substance or ratio between mass and volume. It measures material of a substance in a unit volume. Mathematically, it can be written as:

$$\rho = \frac{m_1}{\nu_1}. \tag{2.10}$$

Here ρ denotes density, m_1 is mass and v_1 is a volume of a substance. Its SI unit is $\frac{ki\log ram}{meter^3}$.

2.7 Pressure

Force exerted on a surface per unit area is identified as pressure. Mathematical expression for the pressure is.

$$P = \frac{F^*}{A}. \tag{2.11}$$

Here P is a pressure, F^* denote force and A is the area of the surface. Its SI unit is pascal which is equal to Nm^{-2}.

2.7.1 Compressible fluid

The fluid having variable density is known as compressible fluid. Density and viscosity of a liquid increases with the increasing of pressure. For example, gas, mercury etc.

2.7.2 Incompressible fluid

The liquid having constant density is known as incompressible fluid. The variation of density in fluid flow with pressure increase or decrease is not high and it can be neglected. For example, air flow through a fan, blood etc.

2.8 Heat

Heat is the flow of energy from a warm object to a cooler object.

2.9 Buoyancy force

The upward force applied by any liquid upon a body set in it is identified as Buoyancy force. Mathematically, it can be expressed as:

$$F_b^* = V_s * D_1 * g_1. \tag{2.12}$$

where F_b^*denote buoyancy force, V_s show the submerged volume, D_1 is the density of fluid and g_1 denotes the force of gravity.

2.10 Concentration

It is a measurement of the amount of a substance in a mixture. It is the ratio of the mass of a substance (M_j) to the total volume of a mixture (V_i). Mathematically, it can be expressed as:

$$C = \frac{M_j}{V_i}. \tag{2.13}$$

Its SI unit is $\frac{ki\log ram}{meter^3}$,and dimension is $\left[\frac{M}{L^3}\right]$.

2.11 Shear thinning

It is the Non-Newtonian conduct of liquids whose thickness diminishes under shear strian. For example: blood, paint, and ketchup.

2.12 Shear thickning

It is the Non-Newtonian conduct of liquids whose thickness increases under shear strian. For example: mixture of cornstarch and water.

2.13 Nanofluid

Nanofluid is an effective heat transfer fluid containing a mixture of Nano-particles (Nanoparticles: Fe, Cu,1-100nm in size) and Base-fluid (base fluid: DI-water, Ethylene, glycol, oil). It increases the thermal conductivity and convective heat transfer coefficient of the base fluid.

2.14 Casson fluid

Casson fluid is characterized as a shear thinning fluid which is expected to have an infinity viscosity at zero rate of shear, a yield stress beneath which no flow happen and a zero viscosity at an infinite rate of shear. For example: honey, jelly, sauce, soup etc.

2.15 Convective boundary condition

This condition is also known as Robins boundary condition, is dened on the surface that both heat conduction and heat convection at the sheet are equal and in the same direction. Mathematically, it can be expressed as:

$$-k\frac{dT(0,t)}{dx} = h[T_{\infty,1} - T(0,t)]. \tag{2.14}$$

2.16 Mechanism of heat transfer

It is a type of energy that move from hotter to colder systems. It is classified into three types.

2.16.1 Conduction

In this type of mechanism of heat transit, direct heat flows from one substance to another due to the collision of unconditional molecules and electrons in liquids and solids. For example ice melting in our hand. Its mathematicall denotation is:

$$Q = -KA\Delta T = -KA(\frac{dt}{dx}). \tag{2.15}$$

Here, negative sign denoting the flow from higher to lower area.

2.16.2 Radiation

In this mechanism of heat transit, heat flow from hotter to colder region due to electromagnetic waves. Its mathematical denotation is:

$$q = e\sigma A(\Delta T)^4. \tag{2.16}$$

2.16.3 Convection

In this mechanism of heat transit, direct heat move from a liquid. Air is a liquid.For example green house effect. Mathematically it can be written as.

$$Q = HA(T_{sys} - T_{\inf}). \tag{2.17}$$

2.17 Thermal conductivity

Measurement of the capacity of substance to conduct heat is known as thermal conductivity.

2.18 Diffusion

The net development of particles from high concentration to low concentration is identified as diffusion.

2.18.1 Brownian diffusion

The nanoparticles that have random movement in the Nanofluid with diameter less than 100nm is called Brownian motion.

2.19 Magnetohydrodynamics(MHD)

Magnetic impact of fluid under electric conduction is known as Magnetohydrodynamics.

2.20 Thermal radiation

In matter, the thermal motion of particles produces electromagnetic radiation is known as thermal radiation.

2.21 Tangent hyperbolic fluid

It is one of the non-Newtonian liquid having four constant fluid models capable of describing shear thinning effect. This fluid has numerous applications in industry and their experimental/ investigational results are considerably utilized in one of a kind laboratories for the reason of industries and engineering.

2.22 Darcy law

Darcy law describes the flow of liquid through spongy/porous media, and it expresses that heat is directly proportional to the permeability of spongy medium K^*, cross-sectional area A, pressure drop ΔP and is inversely proportional to the dynamic viscosity μ.

$$Q = -\frac{K^* A}{\mu}(\Delta P), \tag{2.18}$$

or

$$\Delta P = P_2 - P_1 = -\left(\frac{Q}{A}\right)\frac{\mu}{K^*}, \tag{2.19}$$

or

$$\Delta P = -\frac{\mu}{K^*}q, \tag{2.20}$$

In case of fluid flow $q = v$ (velocity of fluid):

$$\Delta P = -\frac{\mu}{K^*}\nu. \tag{2.21}$$

Negative sign is due to the direction of liquid flow from high pressure towards low pressure region.

2.22.1 Darcy Forchheimer

In Darcy Forchheimer the fluid flow through spongy surface, the viscous forces of fluid prevails the inertial forces and this result in greater flow rate of fluid. The additive term inertial effects/velocity square term is called Forchheimer term which describe the non-linear conduct of pressure difference against data flow. Mathematically, it can be expressed as:

$$\frac{\partial P}{\partial X} = -\frac{\mu}{K}\nu - \frac{\rho_f C_b}{\sqrt{K}}\nu^2. \tag{2.22}$$

2.23 Melting heat

It is a physical action where substance changed over to liquids from solids and stage adjustment happens with an addition in internal energy.

2.24 Dimensionless numbers

2.24.1 Reynolds number (Re)

The significant dimensionaless number which is used to recognize that either the flow is laminar or is turbulent. It describes inertial to viscous forces ratio. Mathematically, it can be expressed as:

$$\mathrm{Re} = \frac{\text{inertial forces}}{\text{viscous forces}}, \tag{2.23}$$

$$\mathrm{Re} = \frac{\nu \times L}{\nu}. \tag{2.24}$$

Here, ν depict the velocity of fluid, L describe the characteristic length and ν represent kinematic viscosity. Reynolds number are utilized to describe distinct flow behavior (laminar or turbulent flow) within a similar fluid. Laminar flow arises at small Reynolds number, in which we can note that viscous effects are eminent. Turbulent flow arises at high Reynolds number where inertial effects are eminent.

2.24.2 Prandtl number (Pr)

It is a dimensionless amount used in computation of heat transfer between a moving fluid and a solid body and is mathematically denoted as;

$$\mathrm{Pr} = \frac{\nu}{\alpha}. \tag{2.25}$$

2.24.3 Skin friction number (C_{fx})

The drag among liquid and solid surface, experienced by a liquid during flow over a surface, is identified as Skin friction coeficient and is additionally causing decrease in the rate of flow.

2.24.4 Schmidt number (Sc)

It is a dimensionless amount used in the ratio of non-Newtonian viscosity (kinematic) to mass diffusivity. Mathematically, it can be written as:

$$Sc = \frac{\nu}{D_B}. \tag{2.26}$$

2.24.5 Nusselt number (Nu_z)

It is a dimensionless amount that corresponds to convection and conduction heat transit parameters at the boundary. Its mathematical expression is:

$$Nu_z = \frac{zq_w}{k\left(T_f - T_\infty\right)}. \tag{2.27}$$

2.24.6 Sherwood number (Sh_z)

It is a dimensionless amount and is the ratio of the convective mass transfer to the rate of diffusivity of mass transport. Mathematically, shown as:

$$Sh_z = \frac{zh_m}{D_B\left(C_f - C\infty\right)}. \tag{2.28}$$

2.24.7 Thermophoresis parameter (N_t)

Thermophoresis is the movement of suspended particles through a fluid affected by an applied thermal gradient. Mathematically shown as:

$$Nt = \frac{\tau D_T\left(T_f - T_\infty\right)}{\nu T_\infty}. \tag{2.29}$$

2.24.8 Hartman number (M)

The ratio between electromagnetic force to the viscous force is identified as Hartman number. Mathematically, expressed as:

$$M = \frac{\sigma B_0^2 l}{\rho U_0}. \tag{2.30}$$

2.24.9 Forchheimer number (F_1)

The Forchheimer number is the ratio of pressure gradient to viscous resistivity. Mathematically, it can be shown as:

$$F_1 = \frac{c_b}{\sqrt{k_1}} z. \tag{2.31}$$

2.24.10 Melting parameter (M_1)

The combination of two stefen quantities $\left(\frac{c_f(T_{\inf}-T_m)}{\lambda}\right)$ and $\left(\frac{c_f(T_m-To)}{\lambda}\right)$ in case of solid and liquid facts. Mathematically, shown as:

$$M_1 = \frac{c_f\left(T_f - T_\infty\right)}{\lambda^* + C_s\left(T_m - T_0\right)}. \tag{2.32}$$

2.25 Homotopic solutions

Homotopy is one of the basic concept of topology. It is stated as continous mapping in which one function can be constantly transformed into the another function. If one function h_1 and the other h_2 are maps from the topological space D with the other topological space E, then there exists a continous mapping H such that

$$H : D \times [0\ , 1] \to E, \tag{2.33}$$

where $d \in D$ and

$$F(d, 0) = h_1(x), \tag{2.34}$$

$$F(d, 1) = h_2(x). \tag{2.35}$$

That mapping H is termed as homotopy.

2.26 Homotopy analysis method

The Homotopy Analysis method (HAM) is involved to find the series solutions of highly nonlinear problems. This method presents us with convergent series solutions for highly nonlinear systems.

Chapter 3

Mixed convection flow of Casson nanofluid over a stretching cylinder with convective boundary conditions

In this chapter we discussed the mass conditions as well as convectional heat with nanoparticles in mixed convection. Flow obey constitutive relationship of casson fluid is initiated through stretched cylinder. Liquid is electrically conducted in the presence of applied magnetic field. The required boundary layer equations is converted into ordinary differential equation after applying some similitude transformation. Homotopy Analysis method is used for the convergent solution of the resulting system. Sherwood numbers and Nusselt number are reduced in term of thermophoresis number.

3.1 Mathematical formulation

We consider an incompressible Casson nanofluid flow bounded by stretched cylinder in presence of convective boundary conditions. The existence of magnetic field does not effect the fluid electric conductivity. In radial direction r-axis is deliberated while alongside the axis of cylinder, z-axis is taken into consideration. The uniform magnetic

field whose intensity is denoted by B_0 act in the radial direction. Here thermal radiation and viscous dissipation are not present. Chemical reaction is ignored in concentration equation. Here u and w are velocities, u along z-direction and w along r direction. T denotes the temperature of fluid and C is fluid concentration. Similarly T_∞ represents the ambient temperature and C_∞ represents the ambient concentration is shown in Fig 3.1.

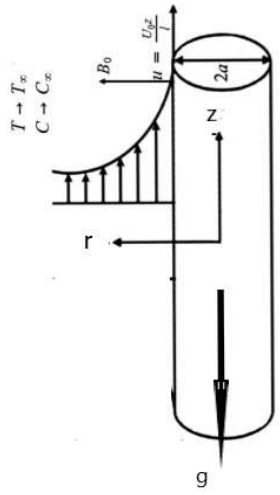

Fig 3.1: Fluid geometry

The subsequent governing equation is assumed as:

$$\frac{\partial u}{\partial z} + \frac{w}{r} + \frac{\partial w}{\partial r} = 0, \tag{3.1}$$

$$u\frac{\partial u}{\partial z} + w\frac{\partial u}{\partial r} = \nu\left(1 + \frac{1}{\beta}\right)\left(\frac{\partial^2 u}{\partial r^2} + \frac{1}{r}\frac{\partial u}{\partial r}\right) +$$

$$g\left[\beta_T\left(T - T_\infty\right)\left(1 - C_\infty\right) + \frac{\left(\rho^* - \rho\right)}{\rho}\left(C - C_\infty\right)\right] - \frac{\sigma B_0^2 u}{\rho}, \tag{3.2}$$

$$u\frac{\partial T}{\partial z} + w\frac{\partial T}{\partial r} = \alpha\left(\frac{\partial^2 T}{\partial r^2} + \frac{1}{r}\frac{\partial T}{\partial r}\right) + \tau\left[D_B\frac{\partial T}{\partial r}\,\frac{\partial C}{\partial r} + \frac{D_T}{T_\infty}\left(\frac{\partial T}{\partial r}\right)^2\right], \tag{3.3}$$

$$u\frac{\partial C}{\partial z} + w\frac{\partial C}{\partial r} = D_B\left(\frac{\partial^2 C}{\partial r^2} + \frac{1}{r}\frac{\partial C}{\partial r}\right) + \frac{D_T}{T_\infty}\left(\frac{\partial^2 T}{\partial r^2} + \frac{1}{r}\frac{\partial T}{\partial r}\right). \tag{3.4}$$

with the subsequent boundary conditions that support the system of equations $(3.1)-(3.4)$.

$$u = U = \frac{U_0 z}{l},\ v = 0,\ -k\frac{\partial T}{\partial r} = h\left(T_f - T\right),$$

$$-D_m\frac{\partial C}{\partial r} = k_m\ \left(C_f - C\right)\ \text{at } r = a,$$

$$u \to 0,\ T \to T_\infty, C \to C_\infty,\ \text{as } r \to \infty. \tag{3.5}$$

Here, dimensionless form of the above mathematical model is obtained by using following transformation

$$u = \frac{1}{r}\frac{\partial \psi}{\psi r},\ w = -\frac{1}{r}\frac{\partial \psi}{\psi z},$$

$$\begin{aligned} \psi &= (U\nu z)^{\frac{1}{2}} af\left(\eta\right),\ \eta = \frac{r^2 - a^2}{2a}\sqrt{\frac{U}{\nu z}}, \\ \theta(\eta) &= \frac{T - T_\infty}{T_f - T_\infty},\ \phi\left(\eta\right) = \frac{C - C_\infty}{C_f - C_\infty}, \end{aligned} \tag{3.6}$$

Here, satisfaction of equation (3.1) is inevitable. However, equations $(3.2)-(3.5)$ reduce to

$$\left(1 + \frac{1}{\beta}\right)\left[\left(1 + 2\gamma\eta\right)f''' + 2\gamma f''\right] + ff'' - f'^2 + \lambda\left[\theta + N_r\phi\right] - Mf' = 0, \tag{3.7}$$

$$\frac{1}{\Pr}\left[\left(1 + 2\gamma\eta\right)\theta'' + 2\gamma\theta'\right] + f\theta' + N_b\left(1 + 2\gamma\eta\right)\theta'\phi' + N_t\left(1 + 2\gamma\eta\right)\theta'^2 = 0, \tag{3.8}$$

$$\left(1 + 2\gamma\eta\right)\phi'' + 2\gamma\phi' + Scf\phi' + \frac{N_t}{N_b}\left[\left(1 + 2\gamma\eta\right)\theta'' + 2\gamma\theta'\right] = 0, \tag{3.9}$$

$$f(0) = 0,\ f'(0) = 1,\ \theta'\left(0\right) = -\gamma_1\left(1 - \theta\left(0\right)\right), \phi'\left(0\right) = -\gamma_2\left(1 - \phi\left(0\right)\right), \tag{3.10}$$

$$f'(\infty) = 0,\ \theta\left(\infty\right) = 0,\ \phi(\infty) = 0. \tag{3.11}$$

with

$$\gamma = \sqrt{\frac{\nu l}{U_0 a^2}},\ \lambda = \frac{gl^2\beta_T}{U_0^2 z}\left(1 - C_\infty\right)\left(T_f - T_\infty\right),\ Nt = \frac{\tau D_T\left(T_f - T_\infty\right)}{\nu T_\infty},$$

$$Nr = \frac{\left(\rho^* - \rho\right)\left(C_f - C_\infty\right)}{\rho\beta_T\left(T_f - T_\infty\right)\left(1 - C_\infty\right)},\ M = \frac{\sigma B_0^2 l}{\rho U_0},\ Nb = \frac{\tau D_B\left(C_f - C_\infty\right)}{\nu},$$

$$\mathrm{Pr} = \frac{\nu}{\alpha},\ Sc = \frac{\nu}{D_B},\ \gamma_1 = \frac{h}{k}\sqrt{\frac{\nu l}{U_0}},\ \gamma_2 = \frac{k_m}{D_m}\sqrt{\frac{\nu l}{U_0}}. \tag{3.12}$$

The Nusselt number and sherwood number in dimensional form is given by:

$$Nu_z = \frac{zq_w}{k(T_f - T_\infty)}, Sh_z = \frac{zh_m}{D_B(C_f - C_\infty)}, \tag{3.13}$$

Here, wall heat flux q_w and wall mass flux h_m is given as:

$$q_w = -k\frac{\partial T}{\partial r}\ |_{r=a}, h_m = -D_B\frac{\partial C}{\partial r}\ |_{r=a}\ . \tag{3.14}$$

Local Nusselt number and local Sherwood number in dimensionless quantities from equations (3.13) and (3.14) are appended as follows:

$$Nu_z\left(\mathrm{Re}_z\right)^{-1/2} = -\theta'\left(0\right), \tag{3.15}$$

$$Sh_z\left(\mathrm{Re}_z\right)^{-1/2} = -\phi'\left(0\right). \tag{3.16}$$

Reynolds number is given as, $\mathrm{Re}_z = \frac{Uz}{\nu}$

3.2 Solution procedure

The method used to find the solution of system is Homotopy analysis method. (HAM) is an analytical technique used to compute the convergent series solutions. This method discriminates itself from other analytical methods due to some important attributes. Following this method, the initial approximations $\left(f_0\left(\eta\right), \theta_0\left(\eta\right), \phi_0\left(\eta\right)\right)$and relevant linear operators $(\mathrm{L}_f\ , \mathrm{L}_\theta,\ \mathrm{L}_\phi)$ are expressed as follows:

$$f_0\left(\eta\right) = [1 - \exp\left(-\eta\right)],$$

$$\theta_0\left(\eta\right) = \left(\frac{\gamma_1}{1+\gamma_1}\right)\cdot\exp\left(-\eta\right),\ \phi_0\left(\eta\right) = \left(\frac{\gamma_2}{1+\gamma_2}\right)\cdot\exp\left(-\eta\right), \tag{3.17}$$

$$\mathrm{L}_f \ = f\,''' - f\,',\ \mathrm{L}_\theta = \theta'' - \theta,\ \mathrm{L}_\phi \ = \phi'' - \phi. \tag{3.18}$$

along with the properties

$$\mathrm{L}_f \ (c_1 + c_2 \exp(\eta) + c_3 \exp(-\eta)) = 0,$$

$$\mathrm{L}_\theta \, (c_4 \exp(\eta) + c_5 \exp(-\eta)) = 0,$$

$$\mathrm{L}_\phi \, (c_6 \exp(\eta) + c_7 \exp(-\eta)) = 0. \tag{3.19}$$

here c_j and $(j = 1 - 7)$ are defined as optional constants.

3.3 Convergence analysis

Homotopy analysis method is applied to determine the convergence solution of non linear system of equations which depends upon supplementary parameters $\hbar_f$, $\hbar_\theta$ and $\hbar_\phi$. These parameters are important to adjust and manage the convergence zone while plotting ħ–curves. The admissible ranges of $\hbar_f$, $\hbar_\theta$ and $\hbar_\phi$ are $-1.1 \leq \hbar_f \leq -0.5$, $-1.4 \leq \hbar_\theta \leq -0.2$ and $-1.3 \leq \hbar_\phi \leq -0.4$. Table 3.1 represents the series solution convergence and it depicts that 30^{th} order of guesstimate is enough to establish the series solution. It can be noticed that the values from table are adequately in order to the H- curves shown in Fig. 3.2.

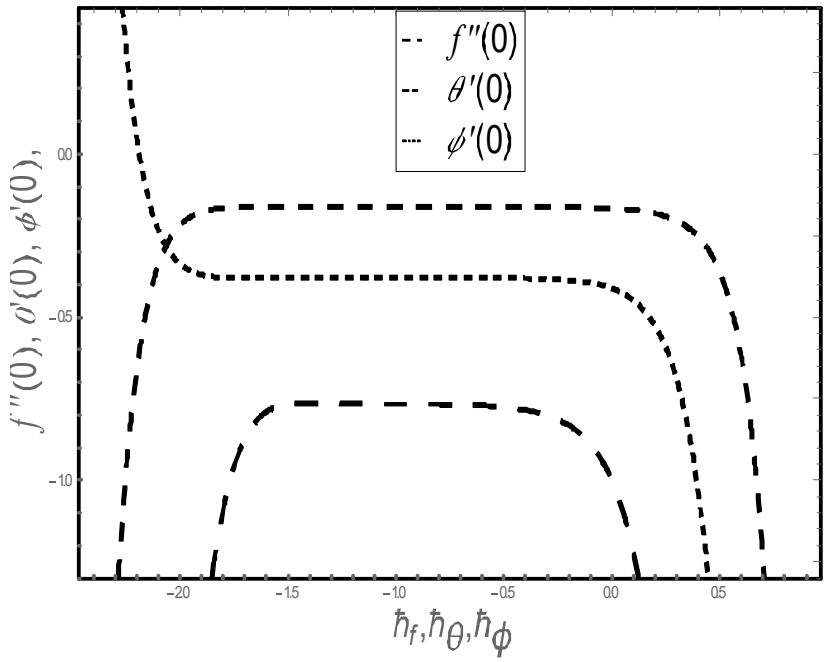

Fig 3.2: ħ-curve for f, θ and ϕ

Table 3.1**:** Convergence of Homotopy series solutions for varied order of estimations.f, θ *and* ϕ.

Order of Approximation	$-f''(0)$	$-\theta'(0)$	$-\phi'(0)$
1	0.87552	0.15903	0.31705
5	0.82354	0.15542	0.28887
10	0.82498	0.15572	0.28845
15	0.82495	0.15570	0.28858
20	0.82493	0.15570	0.28856
25	0.82493	0.15570	0.28856
30	0.82493	0.15570	0.28856

3.4 Results and discussion

The present section clarifies the impacts of distinct parameters on all involved distributions through graphical illustrations. Figures $3.3 - 3.7$ are plotted to determine the

behavior of Casson fluid β, curvature paramter γ, mixed convection number λ, buoyancy number N_r and Hartman parameter M on the velocity profile $f'(\eta)$. In figure 3.3 it is depicted that for greater values of Casson fluid β, velocity gradient decreases. The reason is that the fluid become more viscous with the increasing of Casson fluid. Therefore more resistance is offered which reduces the momentum boundary layer thickness. In figure 3.4 it is seen that for large values of curvature number γ velocity gradient increases, the radius of cylinder decreases which enhance the fluid flow. Figure 3.5, indicates that for growing values of mixed convectional number λ, buoyancy forces enhance, which increase the velocity gradient $f'(\eta)$. Figure 3.6 depicts that for greater number of buoyancy number N_r, velocity gradient increases. Figure 3.7 shows that for greater number of Hartman parameter M, velocity gradient reduces. Figures $3.8-3.11$, plots to depicted the impact of of curvature number γ, Brownian motion number N_b, thermophoresis number N_t, and thermal Biot number γ_1, on the temperature $\theta(\eta)$. Figure 3.8 depicts that for increasing number of curvature number γ, fluid temperature enhances. Figure 3.9 shows that fluid temperature enhances with the greater number of Brownian motion number, which enhance the random motion of nanoparticles. In this process kinetic energy is convert into heat energy due to increment in the collision of nanoparticles. Figure 3.10 shows that for larger number of thermophoresis amount N_t, temperature increases. As thermophoresis causes the small particles to be driven away from a hot surface towards a cold one that's why temperature increases with an increase in N_t. Figure 3.11 depicts that temperature enhances for the greater number of Biot number γ_1. This is because of higher thermal Biot number enhances the heat transfer coefficient and this type of increment in the heat transfer enhances the thermal boundary thickness. Figures $3.12-3.16$ dipicts to examine the behavior of curvature amount γ, Brownian motion amount N_b, thermophoresis parameter N_t, Schmidt parameter Sc, and concentration Biot amount γ_2, on the nanoparticles volume fraction $\phi(\eta)$. In Figure 3.12 it can be noted that for larger values of curvature numbers γ, the volume of nanoparticles enhances. Figure 3.13 dipicts that concentration $\phi(\eta)$ reduces when Brownian motion parameter N_b grows. This is due to the reason

that Brownian motion is a zig zag motion in which the kinetic energy of the particles increases. Which in result shows an increase in particle collision. In this way boundary layer thickness reduces with an increment in N_b. Figure 3.14 dipicts that by increment in the thermophoresis amount N_t, concentration profile $\phi(\eta)$ also reduces. Figure 3.15 shows that by increasing Schmidt amount Sc, the concentration profile $\phi(\eta)$ decreases. Ratio of viscosity to mass diffusivity is known as Schmidt number. When Sc increase then mass diffusivity decreases. Ultimate there is reduction in fluid concentration. Figure 3.16 shows that concentration profile enhances by increasing values of the Biot number γ_2.

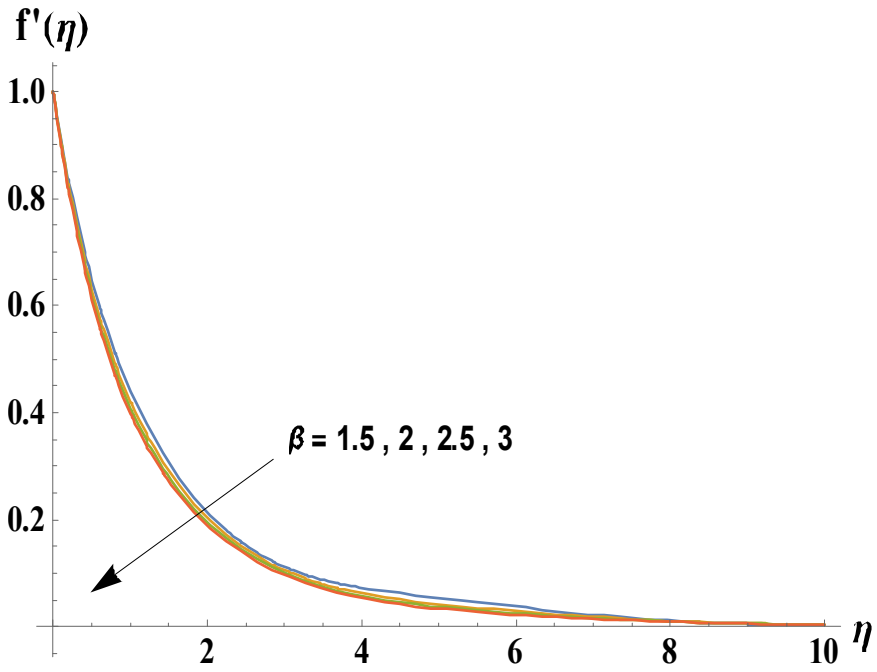

Fig 3.3: Impact of β on $f'(\eta)$

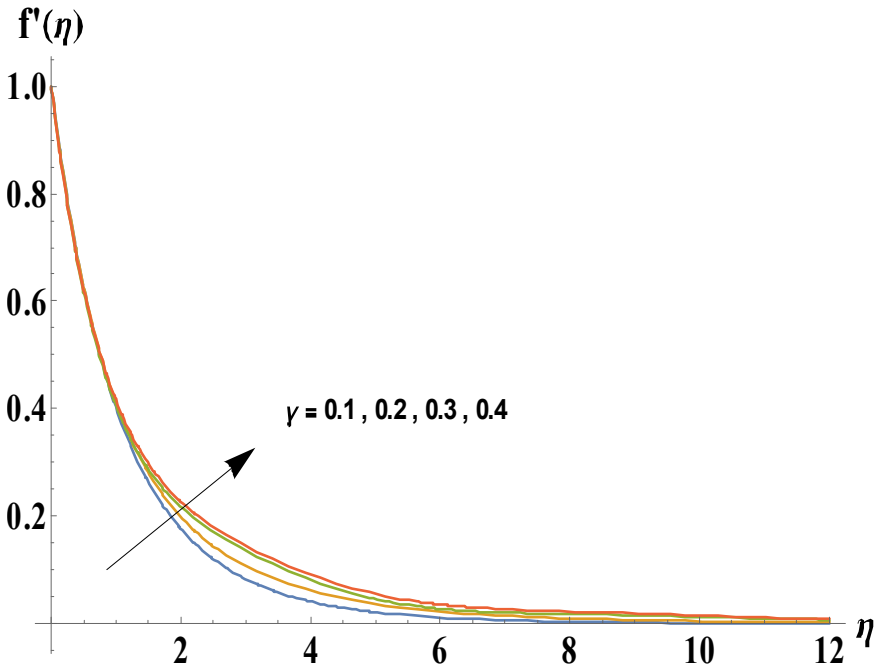

Fig 3.4: Impact of γ on $f'(\eta)$

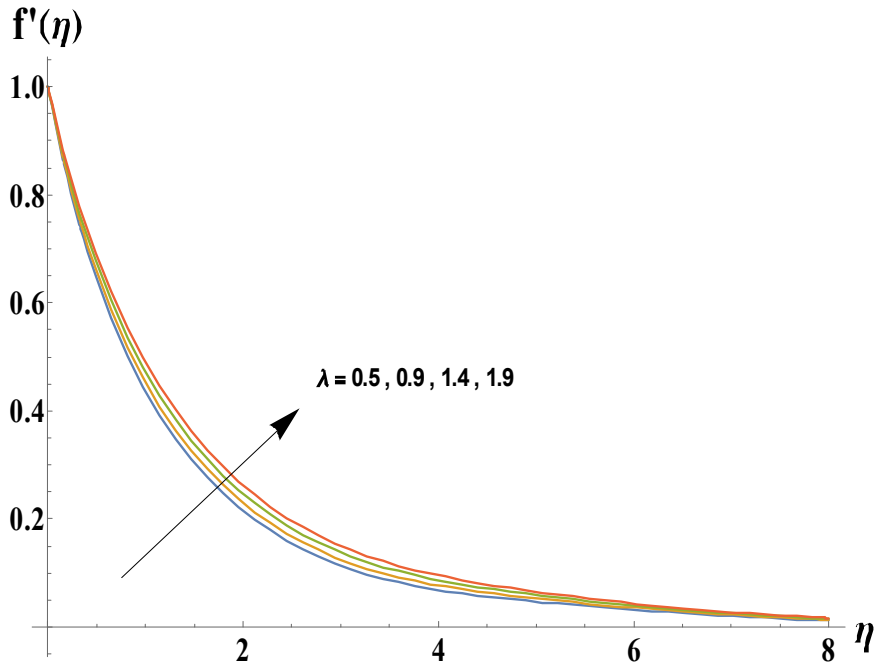

Fig 3.5: Impact of λ on $f'(\eta)$

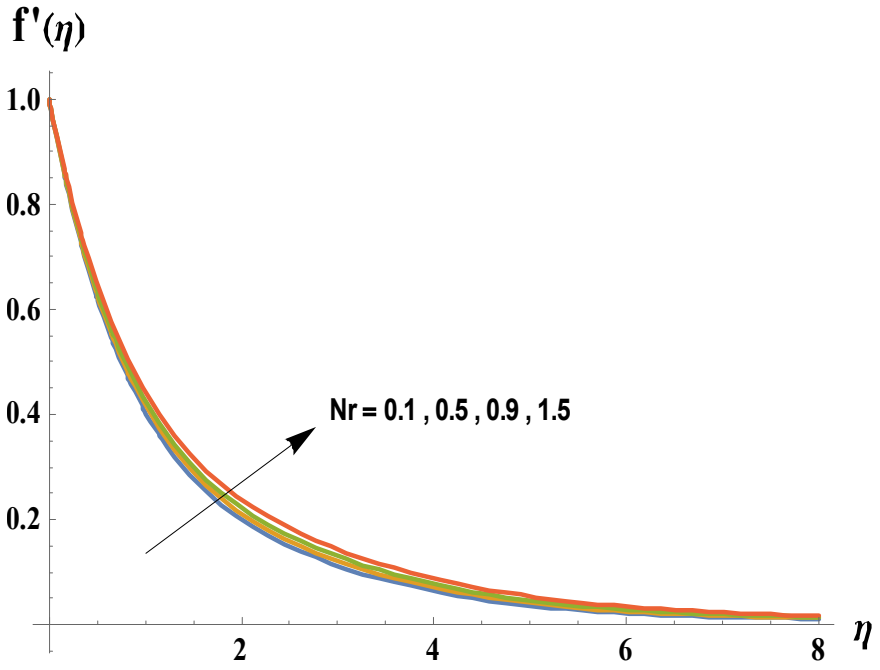

Fig 3.6: Impact of N_r on $f'(\eta)$

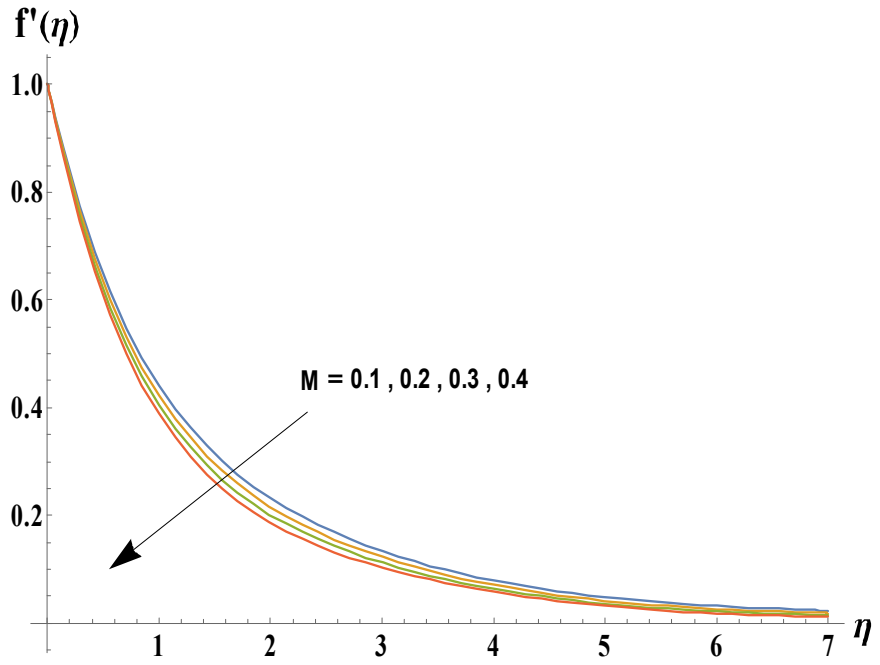

Fig 3.7: Impact of M on $f'(\eta)$

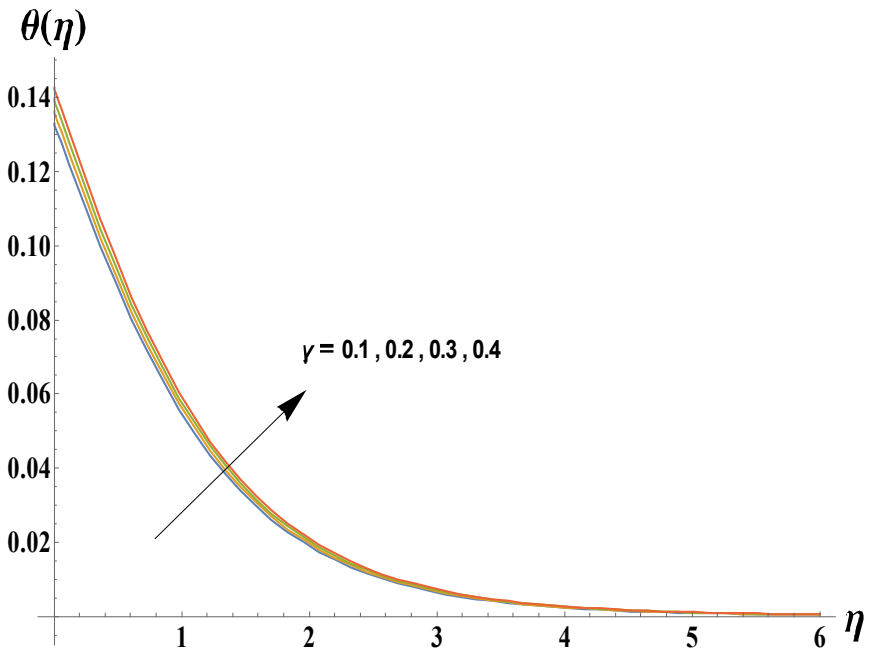

Fig 3.8: Impact of γ on $\theta(\eta)$

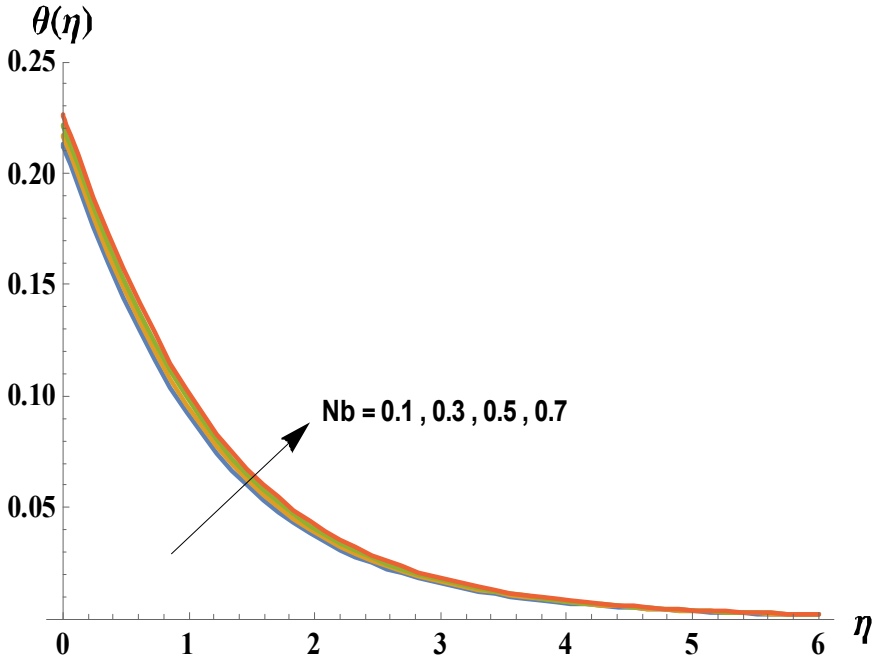

Fig 3.9: Impact of N_b on $\theta\,(\eta)$

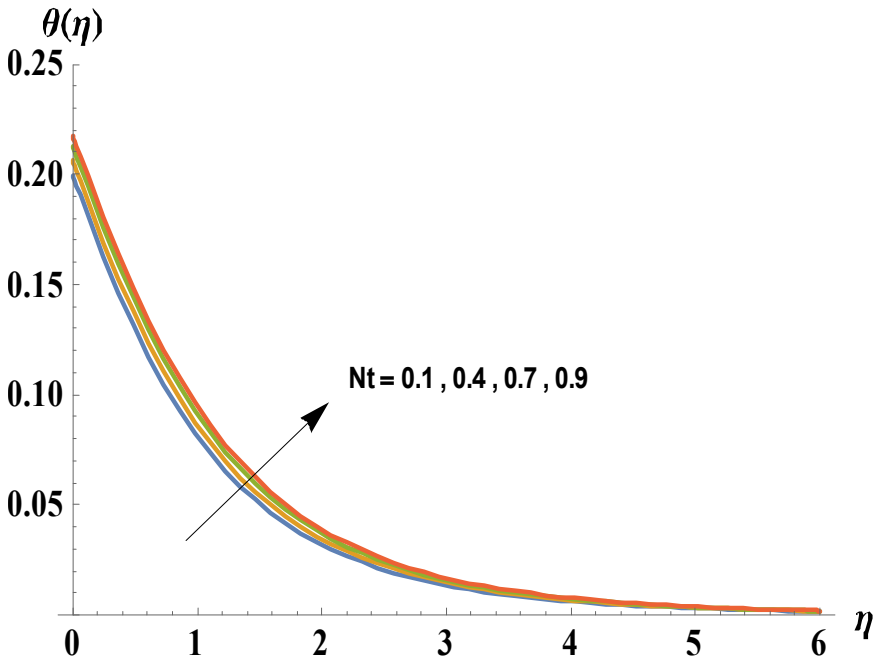

Fig 3.10: Impact of N_t on $\theta(\eta)$

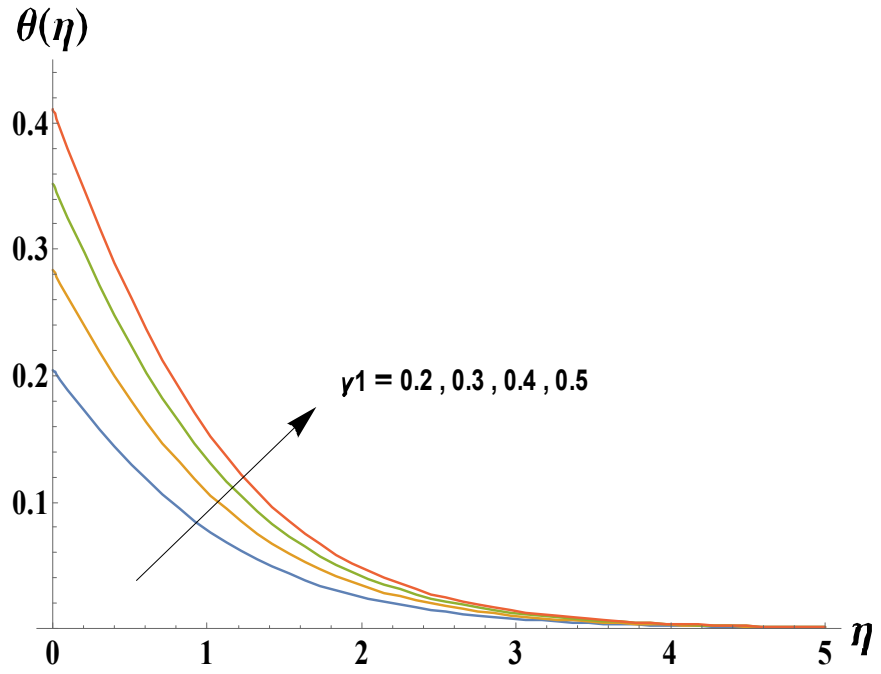

Fig 3.11: Impact of γ_1 on $\theta(\eta)$

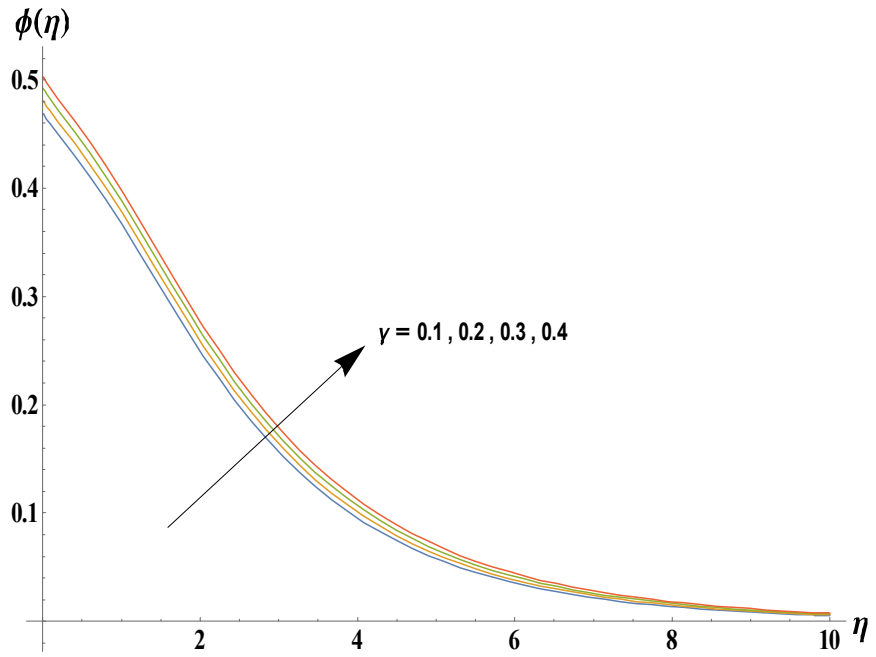

Fig 3.12: Impact of γ on $\phi(\eta)$

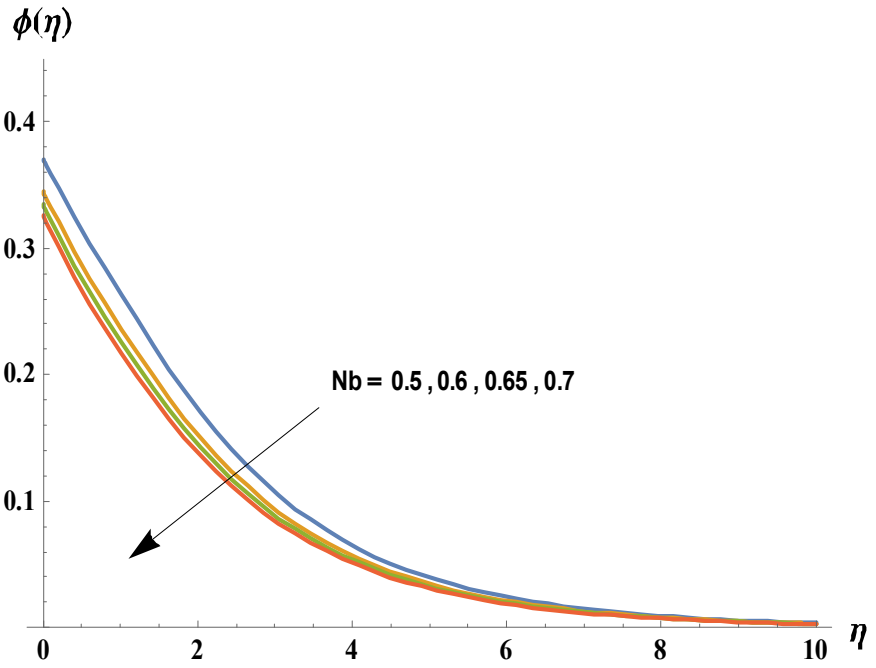

Fig 3.13: Impact of N_b on $\phi(\eta)$

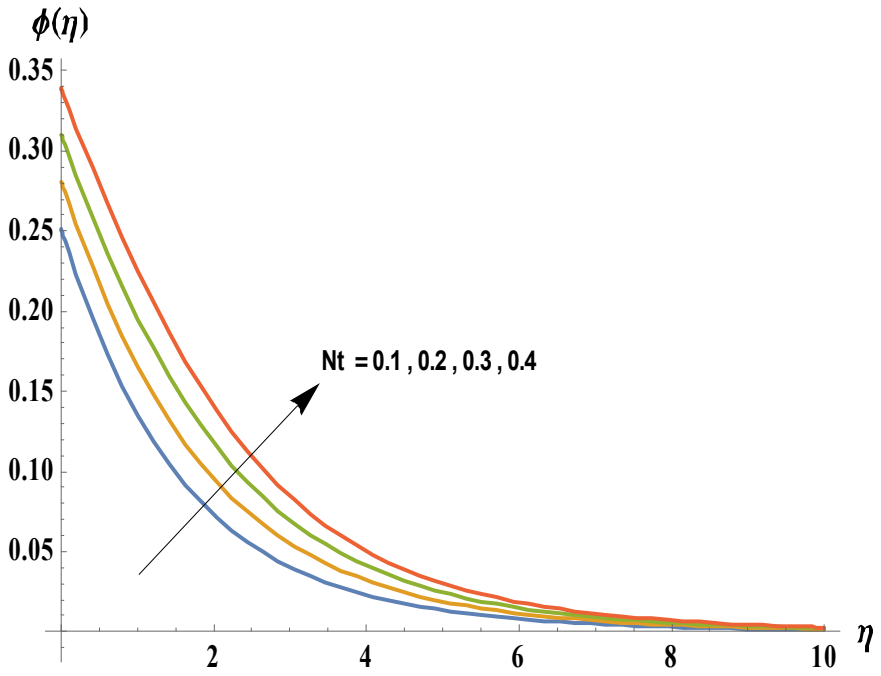

Fig 3.14: Impact of N_t on $\phi(\eta)$

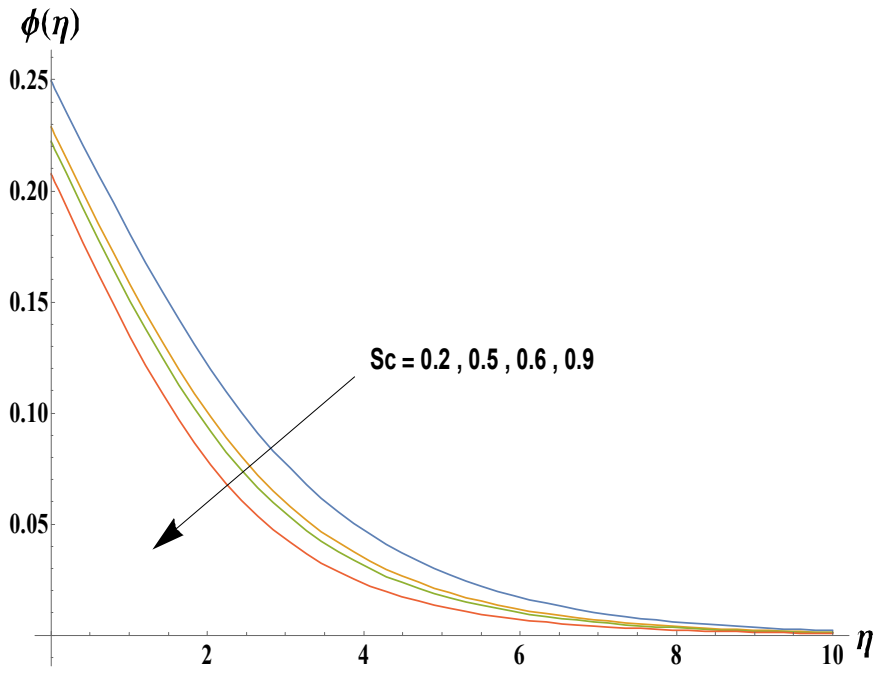

Fig 3.15: Impact of Sc on $\phi(\eta)$

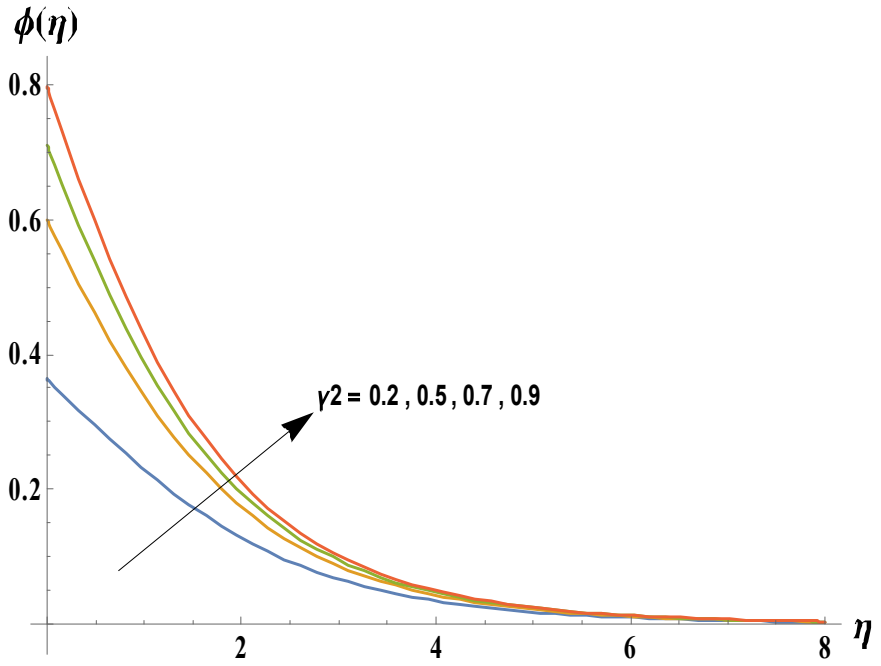

Fig 3.16: Impact of γ_2 on $\phi(\eta)$

Table 3.2 depicts some values of Sherwood numbers and local Nusselt number. Local Nusselt number reduces by growing N_b, N_t, and γ_2 and enhance for greater numbers of

γ and γ_1. Here local sherwood number reduces by growing N_t and γ_1 and enhances for greater numbers of γ, N_b and γ_2.

Table 3.2: Numeric values of Nusselt and sherwood number for different values of $\gamma, N_b, N_t, \gamma_1$,and γ_2.

γ	N_b	N_t	γ_1	γ_2	$Nu_z\,(\mathrm{Re}_z)^{-1/2}$	$Sh_z\,(\mathrm{Re}_z)^{-1/2}$
0.1	0.1	0.1	0.2	0.7	0.15571	0.28856
0.2					0.15712	0.29877
0.3					0.15839	0.30942
0.1	0.2				0.15459	0.31332
	0.3				0.15352	0.32173
	0.4				0.15243	0.32602
	0.1	0.2			0.15553	0.24168
		0.3			0.15532	0.19622
		0.4			0.15513	0.15235
		0.1	0.5		0.29332	0.25090
			0.7		0.35292	0.23510
			0.9		0.39792	0.22329
			0.2	0.5	0.15578	0.24135
				0.8	0.15569	0.30742
				1.0	0.15563	0.33836

Chapter 4

Flow of Tangent hyperbolic nanofluid in Darcy-Forchheimer porous medium over a stretching cylinder with motile gyrotactic microorganism

In this chapter we discussed the convectional heat and mass conditions in the flow of Tangent hyperbolic nanoliquid in a Darcy-Forchheimer porous media over a stretched cylinder with motile gyrotactic microorganism. The liquid is electrically conducted in the behavior of magnetic field. The boundary layer equation is converted into ordinary differential equation after applying some suitable transformation. Built in function bvp4c(MATLAB) is used for the convergent solution of resulting system.

4.1 Mathematical analysis

We consider an incompressible 2-dimensional boundary layer steady laminar flow of Tangent hyperbolic nanofluid in Darcy Forchheimer porous media containing gyrotactic microorganisms. In radial direction r-axis is deliberated while alongside the axis of cylinder, z-axis is taken into consideration. The uniform magnetic field whose intensity is denoted by B_0 act in the radial direction. The magnetic Reynolds number is assumed small and thus the induced magnetic field is negligible in comparison with the applied magnetic field. Electric field effect is not accounted. Here thermal radiation and viscous dissipation are not present. Chemical reaction is ignored in concentration equation.Here C_∞ represents the ambient concentration of fluid and T_∞ is the ambient temperature of fluid as shown in Fig 4.1.

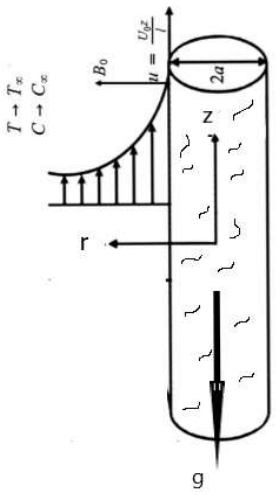

Fig 4.1: Fluid geometry

The governing equations of momentum, energy, mass, and gyrotactic microorganisms in cylinderical coordinates r and z can be written as.

$$\frac{\partial u}{\partial z} + \frac{w}{r} + \frac{\partial w}{\partial r} = 0, \tag{4.1}$$

$$u\frac{\partial u}{\partial z}+w\frac{\partial u}{\partial r}=v\left[\left(1-n^{*}\right)\frac{\partial^{2}u}{\partial r^{2}}+\left(1-n^{*}\right)\frac{1}{r}\frac{\partial u}{\partial r}+n^{*}\sqrt{2}\Gamma\frac{\partial u}{\partial r}\frac{\partial^{2}u}{\partial r^{2}}+\frac{n^{*}\Gamma}{\sqrt{2}r}\left(\frac{\partial u}{\partial r}\right)^{2}\right]$$

$$+g\left[\beta_{T}\left(T-T_{\infty}\right)\left(1-C_{\infty}\right)+\frac{\left(\rho^{*}-\rho\right)}{\rho}\left(C-C_{\infty}\right)-\frac{\left(\rho_{m}-\rho\right)}{\rho}\left(n-n_{\infty}\right)\gamma^{*}\right]-\frac{\nu}{k_{1}}u-$$

$$\frac{C_{b}}{\sqrt{k_{1}}}u^{2}-\frac{\sigma B_{0}^{2}u}{\rho}, \tag{4.2}$$

$$u\frac{\partial T}{\partial z}+w\frac{\partial T}{\partial r}=\alpha\left(\frac{\partial^{2}T}{\partial r^{2}}+\frac{1}{r}\frac{\partial T}{\partial r}\right)+\tau\left[D_{B}\frac{\partial T}{\partial r}\frac{\partial C}{\partial r}+\frac{D_{T}}{T_{\infty}}\left(\frac{\partial T}{\partial r}\right)^{2}\right], \tag{4.3}$$

$$u\frac{\partial C}{\partial z}+w\frac{\partial C}{\partial r}=D_{B}\left(\frac{\partial^{2}C}{\partial r^{2}}+\frac{1}{r}\frac{\partial C}{\partial r}\right)+\frac{D_{T}}{T_{\infty}}\left(\frac{\partial^{2}T}{\partial r^{2}}+\frac{1}{r}\frac{\partial T}{\partial r}\right), \tag{4.4}$$

$$u\frac{\partial n}{\partial z}+w\frac{\partial n}{\partial r}+\frac{bW_{c}}{C_{f}-C_{\infty}}\frac{1}{r}\left[\frac{\partial n}{\partial r}\left(r\frac{\partial C}{\partial r}\right)\right]=D_{n}\frac{1}{r}\frac{\partial}{\partial r}\left(r\frac{\partial n}{\partial r}\right). \tag{4.5}$$

supported by the boundary conditions:

$$u=U=\frac{U_{0}z}{l},\ \nu=0,\ k\frac{\partial T}{\partial r}=\rho\left[\lambda^{*}+C_{s}\left(T_{m}-T_{0}\right)\right]w,$$

$$-D_{m}\frac{\partial C}{\partial r}=k_{m}\left(C_{f}-C\right),n=n_{f}\text{ at }r=a, \tag{4.6}$$

$$u\rightarrow 0,\ T\rightarrow T_{\infty},\ C\rightarrow C_{\infty},\ n\rightarrow n_{\infty},\text{ at }r\rightarrow\infty. \tag{4.7}$$

Here, the subsequent dimensionless transformation are used:

$$u=\frac{1}{r}\frac{\partial\psi}{\partial r},\ w=-\frac{1}{r}\frac{\partial\psi}{\partial z},$$

$$\eta=\frac{r^{2}-a^{2}}{2a}\sqrt{\frac{U}{\nu z}},\ \theta\left(\eta\right)=\frac{T-T_{\infty}}{T_{f}-T_{\infty}},\ \phi\left(\eta\right)=\frac{C-C_{\infty}}{C_{f}-C_{\infty}},$$

$$\psi=\left(U\nu z\right)^{1/2}af\left(\eta\right),\ \chi\left(\eta\right)=\frac{n-n_{\infty}}{n_{f}-n_{\infty}}. \tag{4.8}$$

Here, satisfaction of equation (4.1) is inevitable. However, equations (4.2) − (4.6) take the form:

$$ff''-f'^2+2\gamma\left(1-n^*\right)f''+\left(1-n^*\right)\left(1+2\gamma\eta\right)f'''+2n^*We\left(1+2\gamma\eta\right)^{3/2}f''f'''$$

$$+3n^*We\gamma\left(1+2\gamma\eta\right)^{1/2}f''^2+\lambda\left[\theta\left(\eta\right)+N_r\phi\left(\eta\right)-N_c\chi\left(\eta\right)\right]-Mf'$$

$$-K^*f'-F_1f'^2=0, \tag{4.9}$$

$$\frac{1}{\Pr}\left[\left(1+2\gamma\eta\right)\theta''+2\gamma\theta'\right]+f\theta'$$

$$+N_b\left(1+2\gamma\eta\right)\theta'\phi'+N_t\left(1+2\gamma\eta\right)\theta'^2=0, \tag{4.10}$$

$$\left(1+2\gamma\eta\right)\phi''+2\gamma\phi'+Scf\phi'+$$

$$\frac{N_t}{N_b}\left[\left(1+2\gamma\eta\right)\theta''+2\gamma\theta'\right]=0, \tag{4.11}$$

$$2\gamma\chi'\left(\eta\right)+\left(1+2\gamma\eta\right)\chi''+Lb\Pr f\left(\eta\right)\chi'\left(\eta\right)$$

$$-Pe\left(1+2\gamma\eta\right)\chi'\phi'=0, \tag{4.12}$$

$$f'\left(0\right)=1,\ f\left(0\right)=0,\ M_1\theta'\left(0\right)+\Pr f\left(0\right)=0,\ \phi'\left(0\right)=-\gamma_2\left[1-\phi\left(0\right)\right],$$

$$\chi\left(0\right)=1,\ f'(\infty)\rightarrow 0,\ \theta\left(\infty\right)\rightarrow 0,\ \phi(\infty)\rightarrow 0,\ \chi(\infty)\rightarrow 0. \tag{4.13}$$

with

$$K^*=\frac{\nu}{k_1}\frac{l}{U_0},\ M=\frac{\sigma B_0^2 l}{\rho U_0},\ N_b=\frac{\tau D_B\left(C_f-C_\infty\right)}{\nu},\ \lambda=\frac{gl^2\beta_t}{U_0^2 z}\left(1-C_\infty\right)\left(T_f-T_\infty\right),$$

$$We=\frac{U_0}{l^{3/2}}\sqrt{\frac{U_0}{2\nu}}\Gamma z,\ Lb=\frac{\alpha}{D_n},\ Pe=\frac{bW_c}{D_n},\ M_1=\frac{c_f\left(T_f-T_\infty\right)}{\lambda^*+C_s\left(T_m-T_0\right)},\ F_1=\frac{C_b}{\sqrt{k_1}}z,$$

$$N_c=\frac{\gamma^*\left(\rho_m-\rho\right)\left(n_f-n_\infty\right)}{\rho\beta_t\left(T_f-T_\infty\right)\left(1-C_\infty\right)},\ \alpha=\frac{k}{\rho c_f},\ N_r=\frac{\left(\rho^*-\rho\right)\left(C_f-C_\infty\right)}{\rho\beta_t\left(T_f-T_\infty\right)\left(1-C_\infty\right)},\ \gamma=\left(\frac{\nu l}{U_0a^2}\right)^{1/2},$$

$$\Pr=\frac{\nu}{\alpha},\ N_t=\frac{\tau D_T\left(T_f-T_\infty\right)}{\nu T_\infty},\ Sc=\frac{\nu}{D_B},\ \gamma_2=\frac{k_m}{D_m}\sqrt{\frac{\nu l}{U_0}}. \tag{4.14}$$

The Nusselt number, Sherwood number and density of motile gyrotactic microorganisms in dimensional form is given by:

$$Nu_z = \frac{zq_w}{k(T_f - T_\infty)},\ Sh_z = \frac{zh_m}{D_B(C_f - C_\infty)},\ Nn_z = \frac{zq_n}{D_n(n_f - n_\infty)}. \tag{4.15}$$

Here, wall heat flux q_w, wall mass flux h_m and motile gyrotactic microorganisms flux q_n is given as

$$q_w = -k\frac{\partial T}{\partial r}\ |_{r=a},\ h_m = -D_B\frac{\partial C}{\partial r}\ |_{r=a},\ q_n = -D_n\left(\frac{\partial n}{\partial r}\right)\ |_{r=a.} \tag{4.16}$$

Local Nusselt number, local Sherwood number and density number of motile microorganisms from equation (4.12) and (4.13) in dimensionless form is defined as follows:

$$Nu_z\,(\mathrm{Re}_z)^{-1/2} = -\theta'(0)\,, \tag{4.17}$$

$$Sh_z\,(\mathrm{Re}_z)^{-1/2} = -\phi'(0)\,, \tag{4.18}$$

$$Nn_z\,(\mathrm{Re}_z)^{-1/2} = -\chi'(0)\,. \tag{4.19}$$

$\mathrm{Re}_z = \frac{Uz}{\nu}$ expresses the local Reynolds number.

4.2 Results and discussion

This part is devoted to depict the influenced velocity, temperature, concentration profile and the local density of gyrotax. Various parameters like the curvature number γ, mixed convection number λ, Buoyancy parameter N_r, Hartman number M, Schmidt parameter Sc, Prandtl parameter Pr, Brownian motion number Nb, thermophoresis parameter Nt, concentration Biot number γ_2, Weissenberg number We, local inertia coefficient F_1, porosity parameter K^*, Peclet number Pe, and melting parameter M_1 influenced on velocity profile $f'(\eta)$, temperature, concentration profile ϕ and gyrotax density are discussed and analyzed. In Figure 4.2 it is indicated that greater values of curvature

number γ causes an increment in velocity profile $f'(\eta)$.When curvature parameter γ increase it enhances the radius of cylinder which increase the liquid flow. Features of mixed convection number λ on the velocity $f'(\eta)$ are noticed in Figure 4.3. It is depicted that the velocity profile increases for large number of mixed convection number λ. Figure 4.4 defines the influence of Buoyancy paramter N_r on velocity profile $f'(\eta)$. Velocity profile enhances, for larger N_r. Hartman parameter M on the $f'(\eta)$ is shown in Figure 4.5. It is elucidated that when the values of Hartman parameter M are larger then boundary layer thickness becomes lower. An increment in the power of magnetic field cause resistivity in force, which reduce the velocity of liquid. Figure 4.6 is plotted to show that an influence in Weissenberg number We corresponds to decay in influenced velocity $f'(\eta)$. Due to growing values of Weissenberg number We there is increment in relaxation time which offer more resistance to flow and results in low velocity. Figure 4.7 shows the decrement behavior of the local inertia coefficient F_1 in velocity profile $f'(\eta)$. This is becuase the porous medium slow down the motion of fluid and this result in decreasing of velocity. The desending behavior in velocity distribution $f'(\eta)$ of porosity parameter K^* is noticed in figure 4.8. Figure 4.9 is portrayed to notice the significant aspects of power index n^* on velocity gradient $f'(\eta)$. By increasing the values of power law index n^* the boundary layer thickness decreases. This is due to the fact that fluid nature changes from shear thinning to shear thickning in an increasing n^*. Figure 4.10 portraied the behavior of thermophoresis number N_c on velocity profile $f'(\eta)$. It is noted that velocity profile decays with increasing values of biconvection Rayleigh parameter N_c. N_c parameter involve density difference which creates reduction in velocity profile. Change in temperature gradient $\theta(\eta)$ for the values of curvature parameter γ is sketched in Figure 4.11. The temperature enhences, for large estimates of curvature parameter γ. Figure 4.12 illustrates the variation of Brownian motion amount N_b on temperature profile $\theta(\eta)$. It is seen that for growing values of Brownian motion number N_b temperature profile is enhanced, which enhance the random motion of nanoparticles. In this process kinetic energy is convert into heat energy due to increment in the collision of nanopar-

ticles. Figure 4.13 portraied the behavior of thermophoresis number N_t on temperature profile $\theta(\eta)$. Temperature $\theta(\eta)$ increase for growing values of thermophoresis number N_t. Greater values of thermophoresis number N_t causes an increment in the thermophoretic forces which leads to movement of nanoparticles from hot to cold surfaces and similarly it increases the temperature. Figure 4.14 depicts the temperature field $\theta(\eta)$ for various values of melting parameter M_1. Due to melting process it acts like a blowing boundary condition at the stretched surface of cylinder. By increasing melting parameter the difference between fluid ambient temperature and temperature of the melting surface increases and there is increment in the boundary layer thickness which diminishes the liquid temperature. Figure 4.15 depicts that for increasing values of Brownian motion number N_b cause decrement in concentration profile $\phi(\eta)$. In nanoliquid flow,because of existence of nanoparticles, the Brownian motion occurs and with an increment in the Brownian motion number N_b it is affected and similarly the boundary layer thickness reduces. Figure 4.16 shows the behavior against concentration parameter $\phi(\eta)$. Here, $\phi(\eta)$ is an increasing function of γ. Figure 4.17 is plotted to show the curves of $\phi(\eta)$ for various terms of N_t at other variables are fixed. It can be judged that N_t influences the temperature. Figure 4.18 is plotted to show that an increment in Schmidt amount Sc corresponds to decrement in nanoparticles influenced concentration $\phi(\eta)$. There is an inverse relationship between Schmidt number and the Brownian parameter. Greater number of Schmidt parameter Sc leads to a lower Brownian diffusion coefficient which causes reduction in nanoparticles concentration. This is the reason that a rise in the Sc produce a decay in diffusion coefficient which brings about a reduce in concentration and its associated boundary layer thickness. Figure 4.19 analysis the difference in concentration for various values of concentration Biot amount γ_2. Here we noticed that the concentration is a increasing function of γ_2. Influences of Pe on the gyrotax density is noted in Figure 4.20. It is noted that the gyrotax density decreases for growing values of Pe. Because Pe number has direct relation with cell swimming speed which created decreasing trend in density of motile microorganisms. Figure 4.21 shows an increasing

effect of gyrotax density $\chi(\eta)$ by increasing the number of γ. Figure 4.22 shows an increasing effect of gyrotax density $\chi(\eta)$ by increasing the number of N_b. As the N_b motion number increased the nanoparticles diameter peogressively smaller, it leads to increase in density of microorganisms. Figure 4.23 shows an decreasing effect of gyrotax density $\chi(\eta)$ by increasing the number of L_b. A decrement in $\chi(\eta)$ is achieved for higher bio-convection Lewis number L_b, bio-convection Lewis number has inverse relation with motile microorganism diffusion coefficient which causes decay in the density of motile microorganisms.

Table 4.1 shows the values of Nusselt number and Sherwood number for various parameters. Nusselt number exhibits an increasing behaviour on rising amount of γ, We, M_1,and for power law index n^* while decreasing behavior is noted for N_b, N_t,and γ_2 and sherwood number diminshes for increasing behavior of N_b and increasing for γ, We, M_1, n^*, N_b, N_t, and γ_2.

Table 4.2 displays the impact of Lb, Pe, Pr, γ, We, M_1, N_b, and N_t on density number of motile microorganisms. Density number enhances on increasing values of Lb, Pe, Pr, γ, We, M_1, N_t while diminishes for N_b.

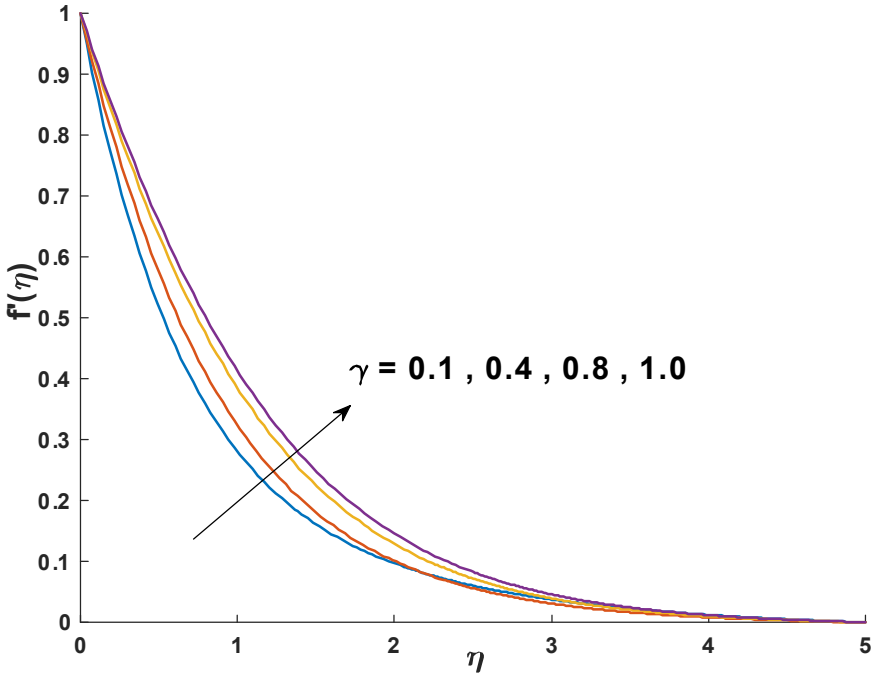

Fig 4.2: Impact of γ on $f'(\eta)$

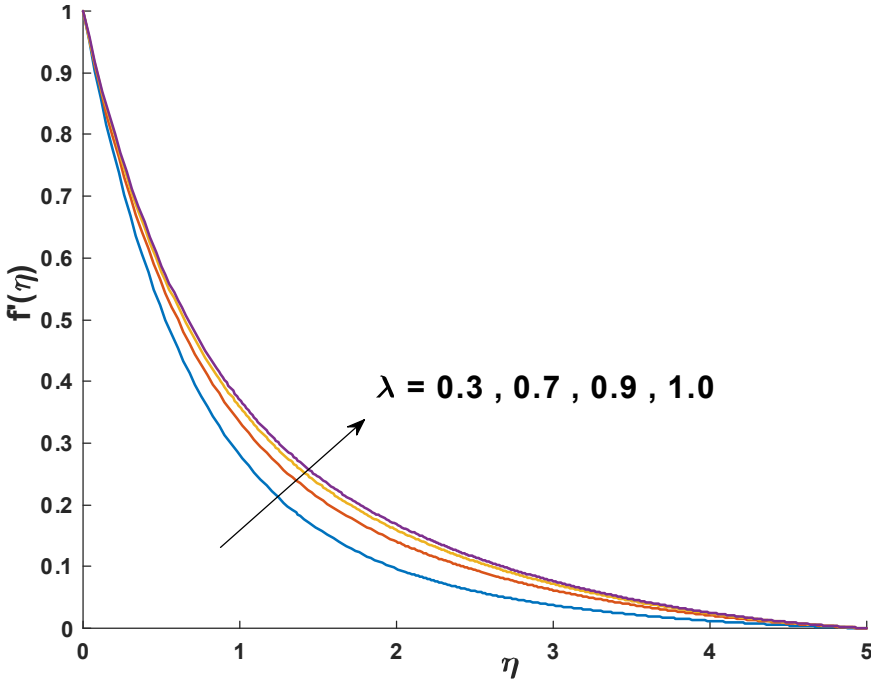

Fig 4.3: Impact of λ on $f'(\eta)$

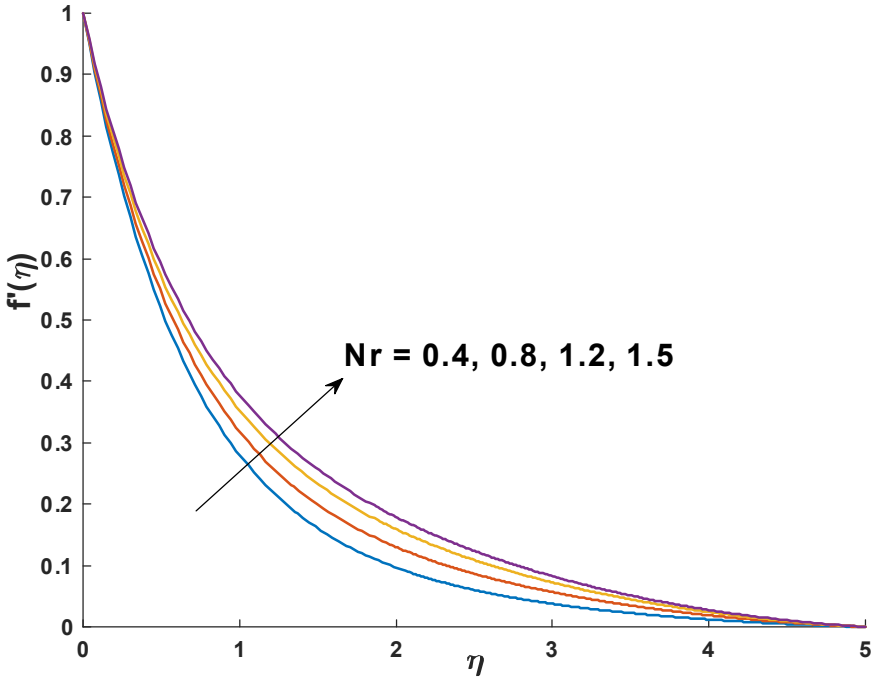

Fig 4.4: Impact of N_r on $f'(\eta)$

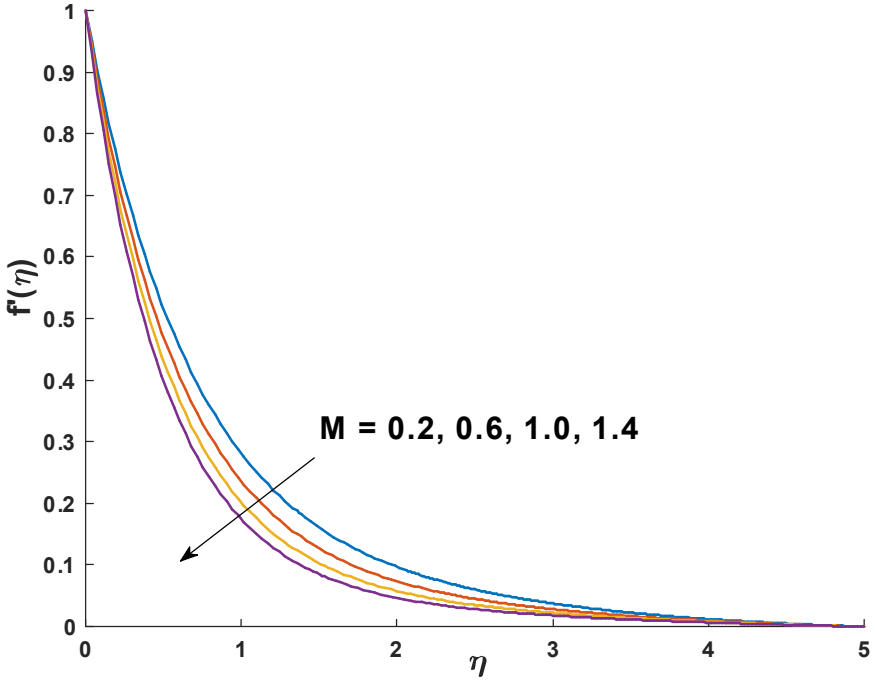

Fig 4.5: Impact of M on $f'(\eta)$

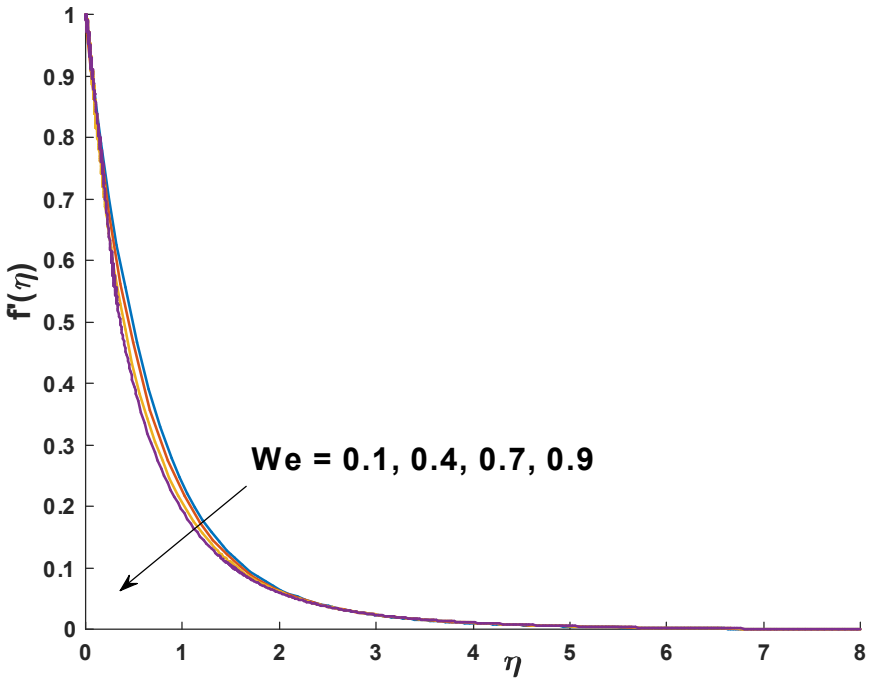

Fig 4.6: Impact of We on $f'(\eta)$

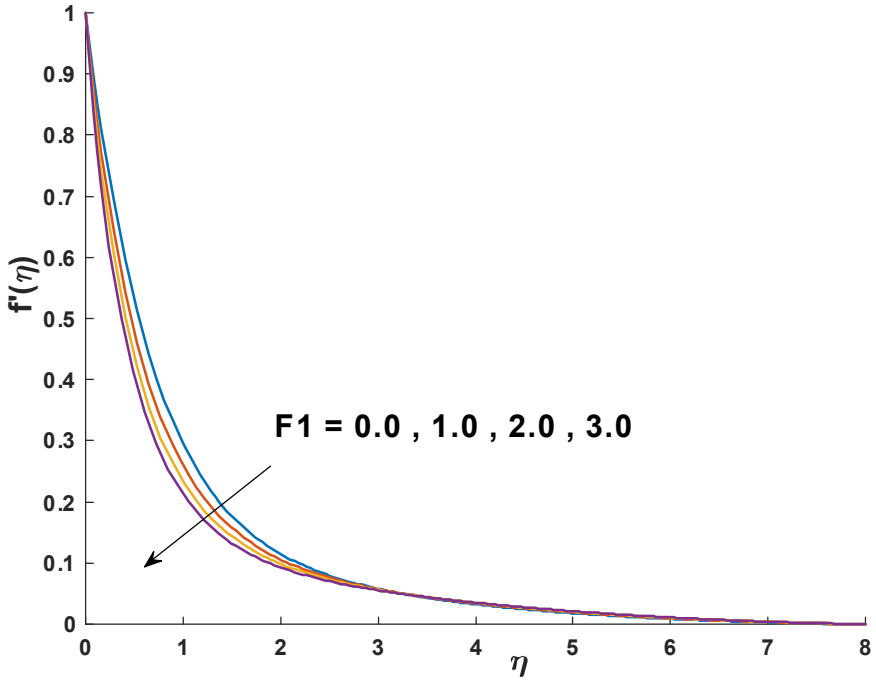

Fig 4.7: Impact of F_1 on $f'(\eta)$

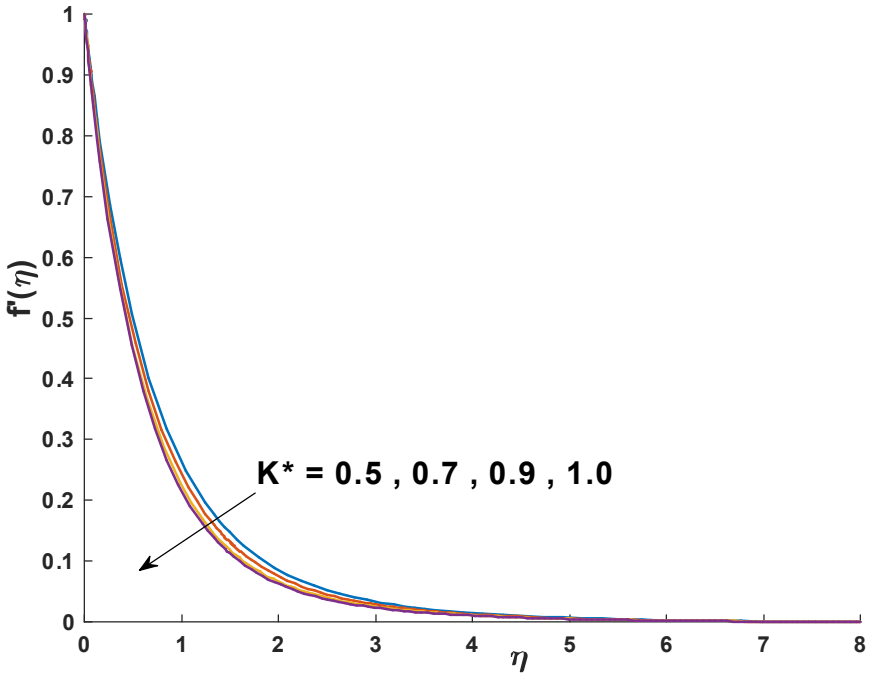

Fig 4.8: Impact of K^* on $f'(\eta)$

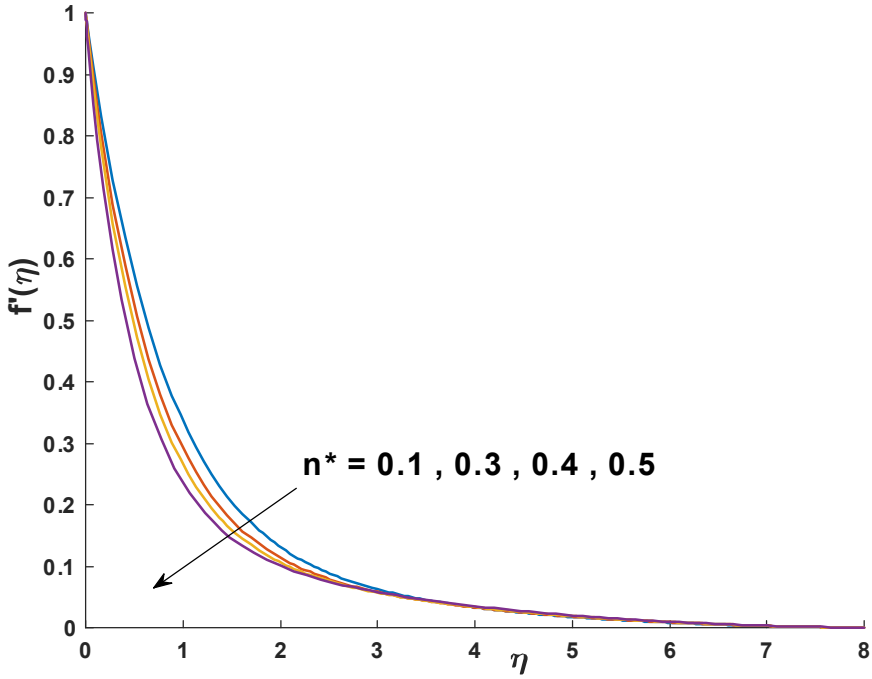

Fig 4.9: Impact of n^* on $f'(\eta)$

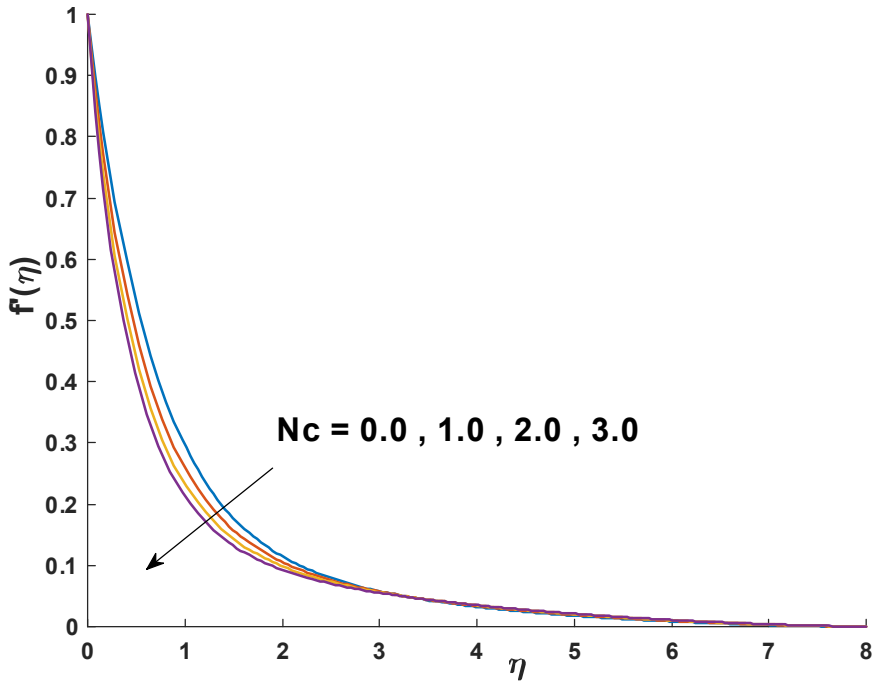

Fig 4.10: Impact of N_c on $f'(\eta)$

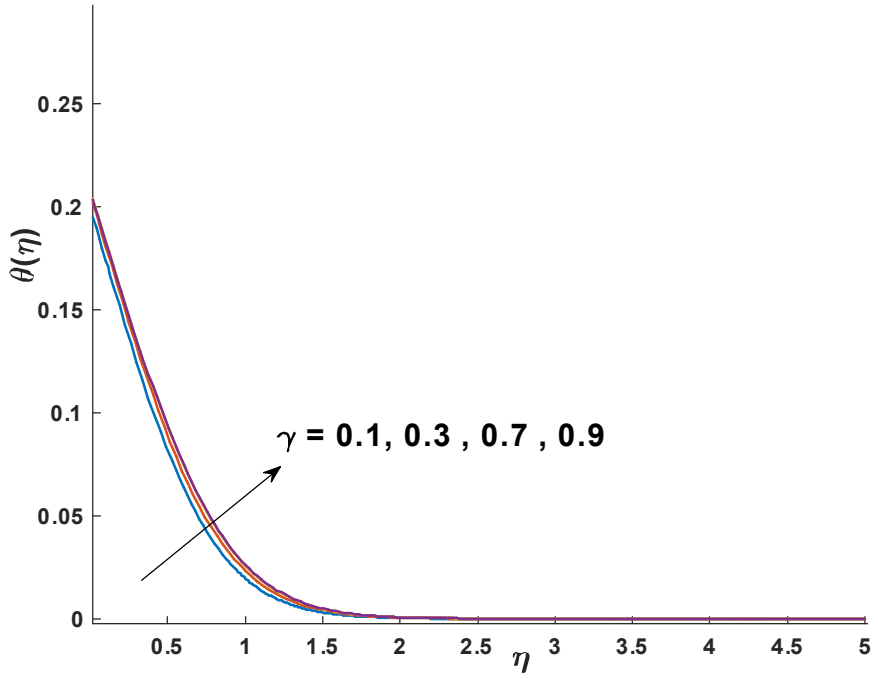

Fig 4.11: Impact of γ on $\theta(\eta)$

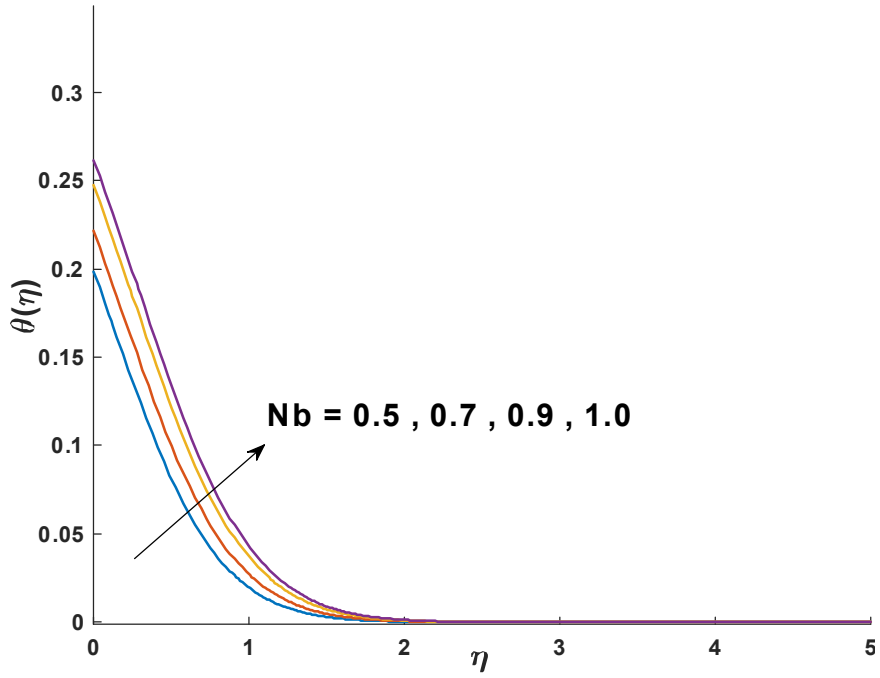

Fig 4.12: Impact of N_b on $\theta(\eta)$

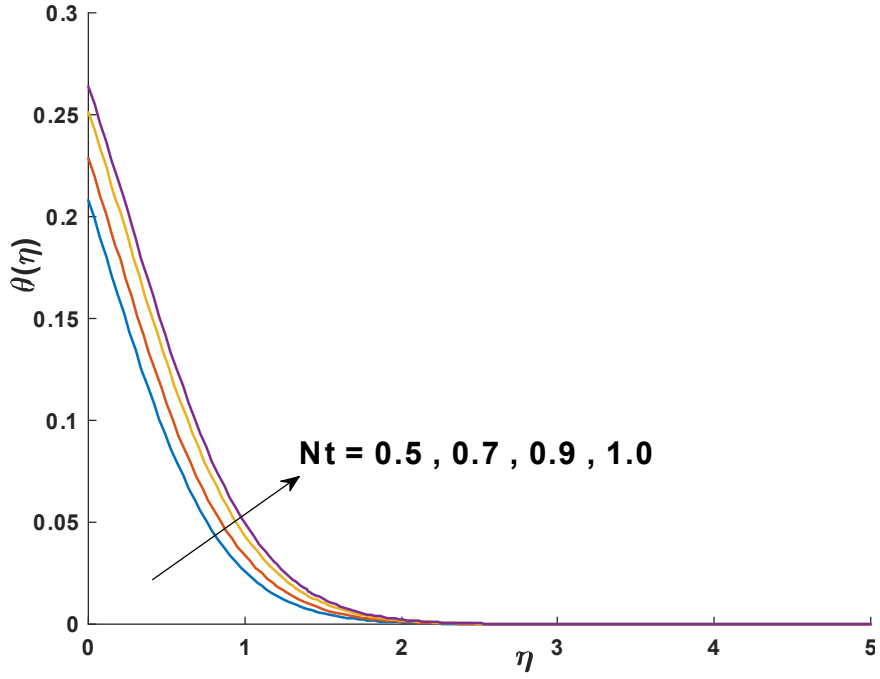

Fig 4.13: Impact of N_t on $\theta(\eta)$

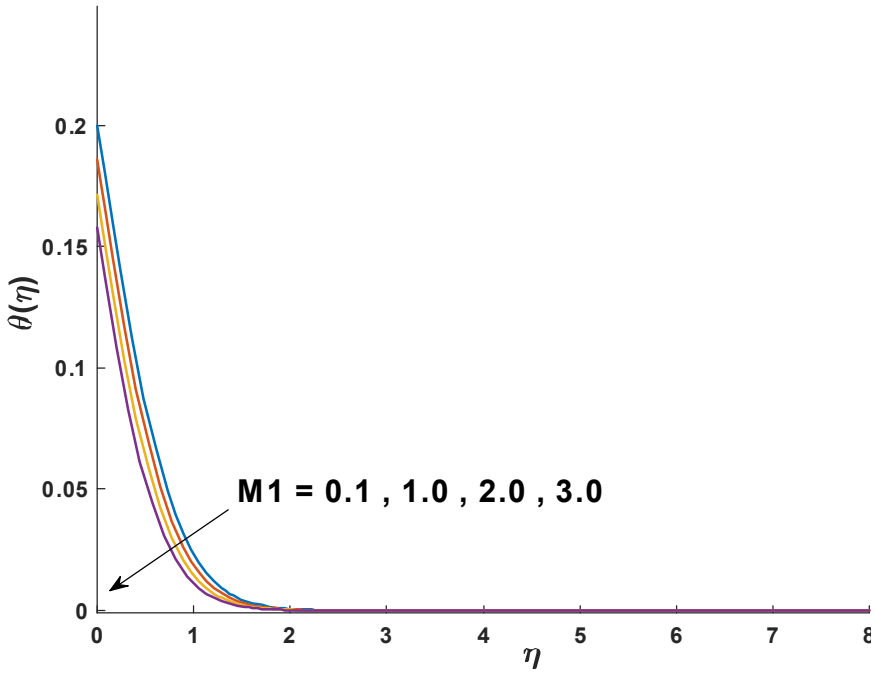

Fig 4.14: Impact of M_1 on $\theta\,(\eta)$

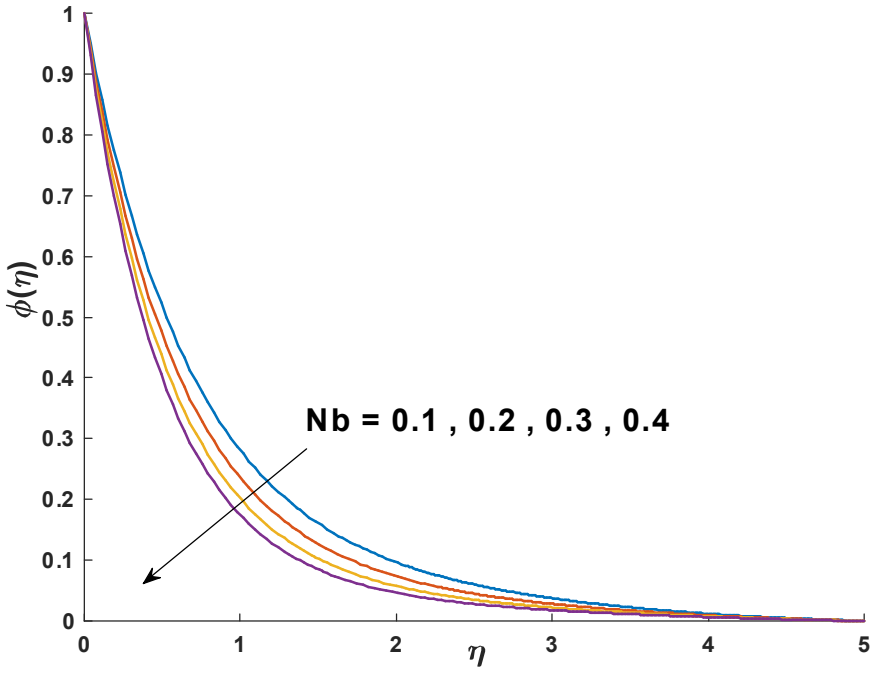

Fig 4.15: Impact of N_b on $\phi\,(\eta)$

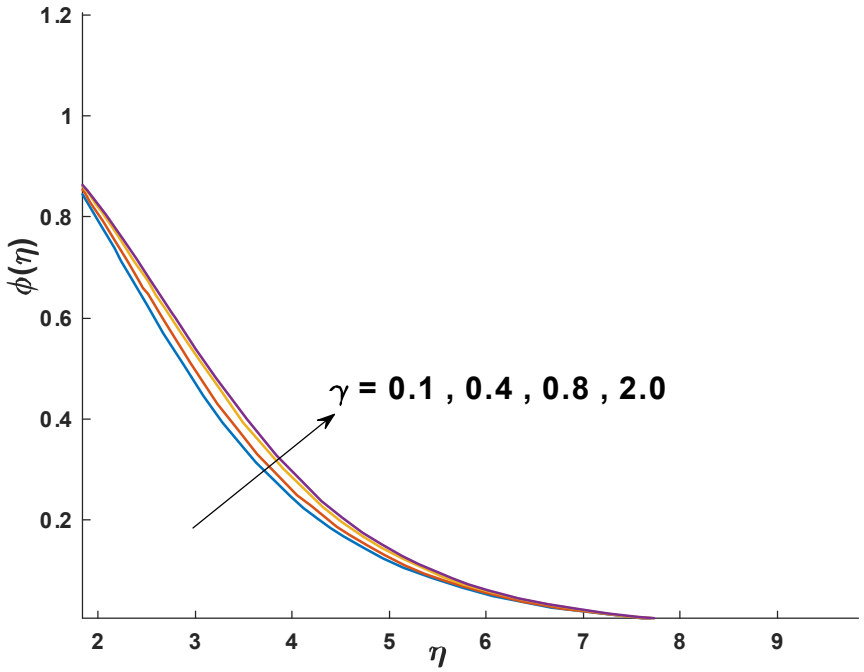

Fig 4.16: Impact of γ on $\phi(\eta)$

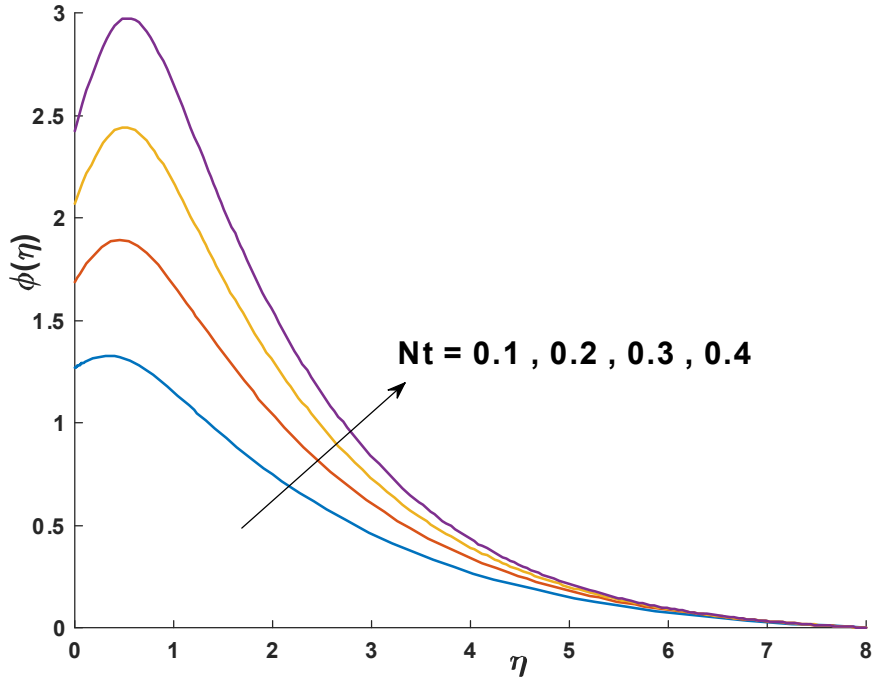

Fig 4.17: Impact of N_t on $\phi(\eta)$

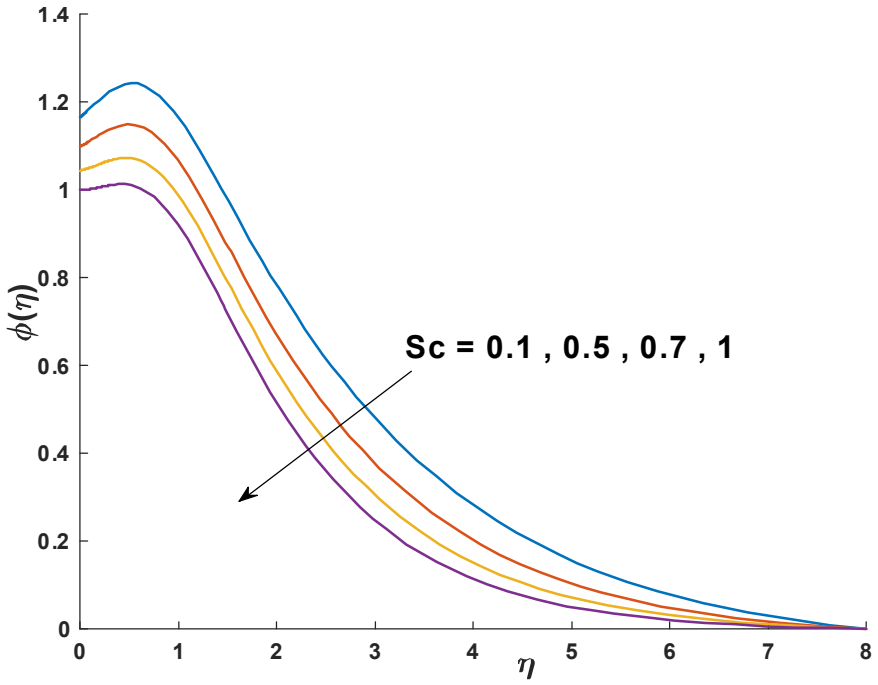

Fig 4.18: Impact of Sc on $\phi(\eta)$

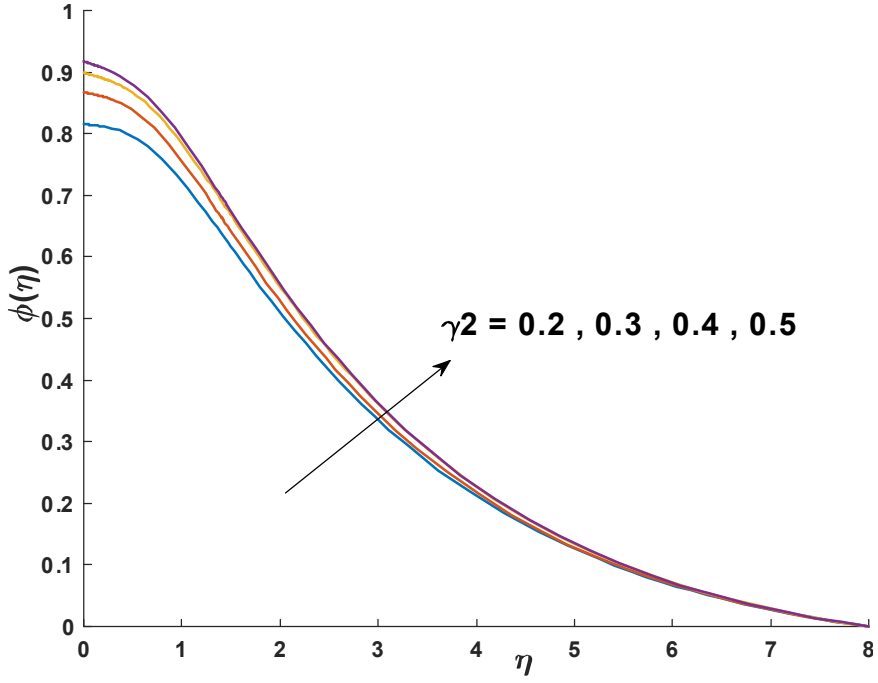

Fig 4.19: Impact of γ_2 on $\phi(\eta)$

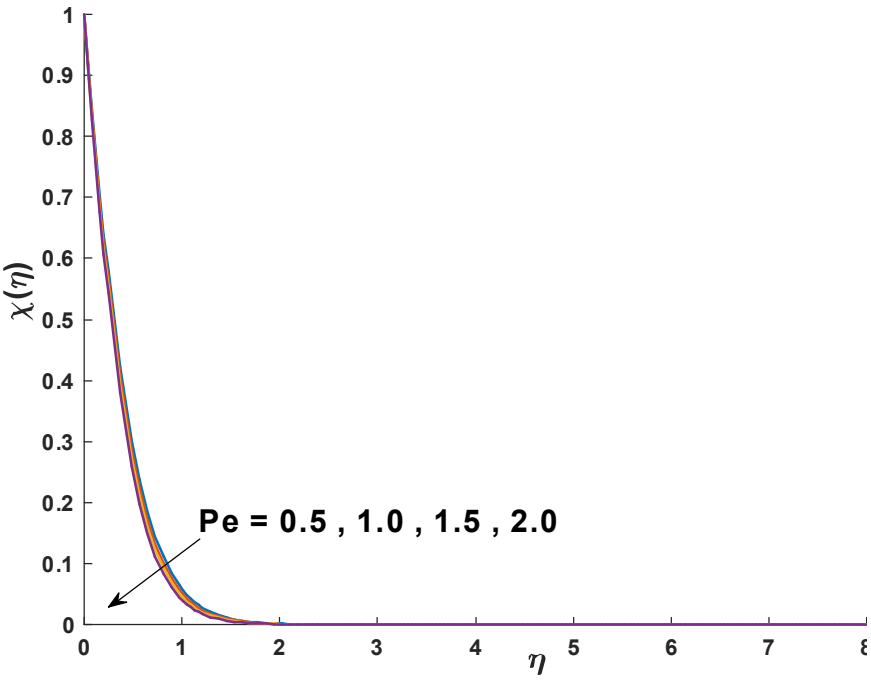

Fig 4.20: Impact of Pe on $\chi(\eta)$

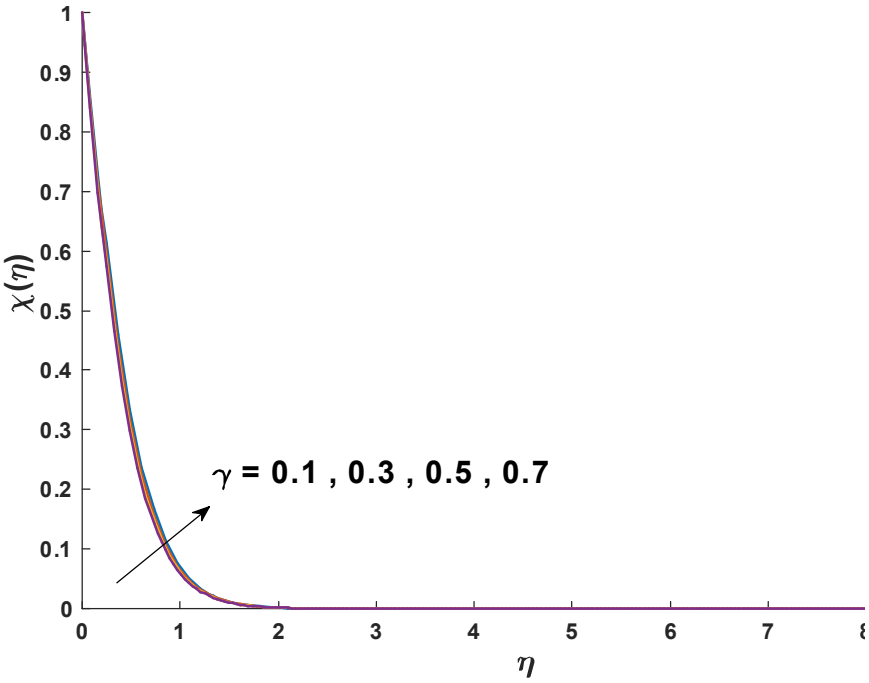

Fig 4.21: Impact of γ on $\chi(\eta)$

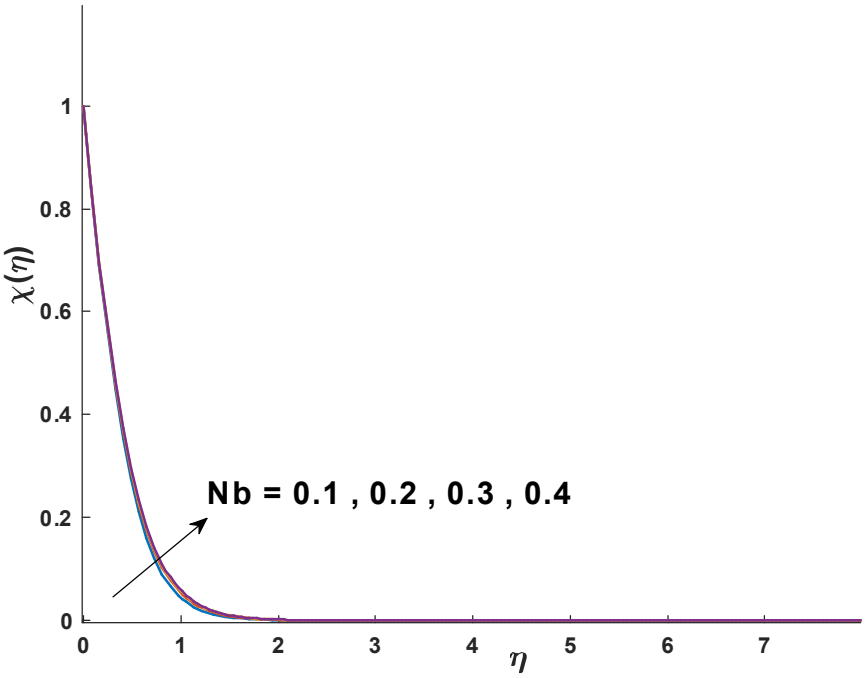

Fig 4.22: Impact of N_b on $\chi(\eta)$

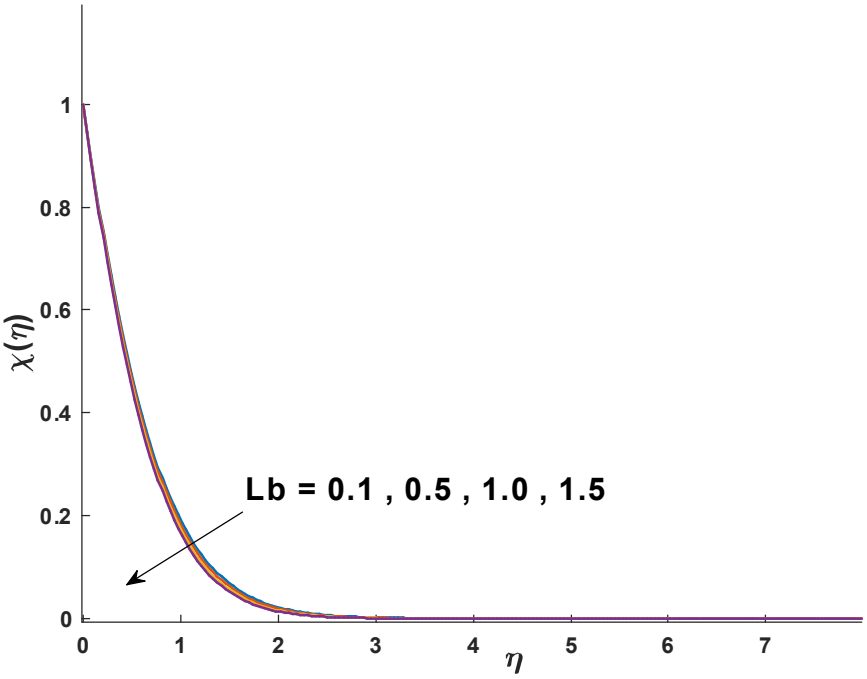

Fig 4.23: Impact of Lb on $\chi(\eta)$

Table 4.1: Numerical values of Nusselt and Sherwood numbers for different values of $\gamma, N_b, N_t, \gamma_2, We, M_1$, and n^*.

γ	N_b	N_t	γ_2	We	M_1	n^*	$Nu_z\,(\mathrm{Re}_z)^{-\frac{1}{2}}$	$Sh_z\,(\mathrm{Re}_z)^{-\frac{1}{2}}$
0.1							0.24449	0.13815
0.2							0.24457	0.18931
0.3							0.24511	0.23598
0.1	0.2						0.17588	0.27756
	0.3						0.17501	0.15546
	0.4						0.17423	0.088754
	0.1	0.2					0.25264	0.10911
		0.3					0.25187	0.25377
		0.4					0.25105	0.39496
		0.1	0.5				0.25337	0.036463
			0.8				0.25333	0.043021
			1.0				0.25331	0.045767
			1.5	1.0			0.64682	0.2417
				1.5			0.6513	0.24469
				1.9			0.68218	0.25131
				1.2	0.5		0.63888	0.24065
					0.7		0.65662	0.24574
					0.9		0.67748	0.25632
					0.6	0.3	0.6487	0.24312
						0.4	0.66156	0.24704
						0.5	0.65885	0.25032

Table 4.2 : Numerical values of density of motile gyrotactic microorganisms for different values of γ, N_b, N_t, We, Pr, M_1, L_b, and Pe.

γ	N_b	N_t	We	Pr	M_1	L_b	Pe	$Nn_z\,(\mathrm{Re}_z)^{-\frac{1}{2}}$
0.1								0.73986
0.2								0.83802
0.3								0.92491
0.1	0.2							0.71345
	0.3							0.71268
	0.4							0.71224
	0.1	0.2						0.73463
		0.3						0.74714
		0.4						0.75803
		0.1	1.0					0.83764
			1.5					0.84552
			1.9					0.93038
			1.2	5				0.77699
				6				0.81437
				7				1.0104
				6	0.5			0.81437
					0.7			0.85871
					0.9			0.90134
					0.6	0.2		0.83976
						0.3		1.057
						0.4		1.2387
						0.2	0.1	0.83976
							0.2	0.8495
							0.3	0.85897

Chapter 5

Conclusions and future work

In this thesis two problems have been analysed where first problem is about review paper and second problem is the extension work for it. Conclusion of both the problems are as followings:

5.1 Chapter 3

The impact of mass condition and convective heat in mixed convection flow of casson nanoliquid by stretch cylinder is discussed in the presence of applied magnetic field. The main consequences of this analysis are listed below:

- Influenced velocity, temperature and nanoparticles concentration are greater for higher amount of curvature number.
- Velocity gradient is decreasing for the greater amount of Hartman parameter and Casson fluid number.
- Temperature enhanced by increasing thermophoresis number and Brownian motion.
- Influenced concentration enhances for the greater values of Biot amount.
- Concentration profile increases for greater values of thermophoresis number.

- Larger values of Schmidt parameter cause a decrement in concentration distributions.

5.2 Chapter 4

- In the present exploration, we have studied the flow of Tangent Hyperbolic nanofluid flow in Darcy-Forchheimer porous media through stretched cylinder with motile gyrotactic microorganisms. Analytical solution of the problem is extracted by using bvp4c(Matlab) method. The salient features of the present investigation are appended as follows:
- Velocity, temperature, local gyrotax density and nanoparticles concentration are higher for higher values of curvature parameter.
- Velocity profile decreases for larger values of Wessenberg number, local inertia coefficient and porosity parameter.
- Temperature reduces for greater values of melting parameter.
- Velocity profile reduces for growing values of power law index.
- Local density of motile microorganisms influenced by increasing Peclet number.

5.3 Future work

The current study can be extended to the subsequent models as well:

- The model may be extended to any other non-Newtonian fluid.
- The energy equation can be enhanced by adding the Cattaneo-Christov heat flux.
- The effect of Arrhenius activation energy can be added.

Bibliography

[1] Gorla, R.S.R. and Hossain, A. (2013) Mixed Convective Boundary Layer Flow over a Vertical Cylinder Embedded in a Porous Medium Saturated with a Nano-fluid. International Journal of Numerical Methods for Heat & Fluid Flow ,23,1393-1405.

[2] Imtiaz, M., Hayat, T., & Alsaedi, A. (2016). Mixed convection flow of Casson nanofluid over a stretching cylinder with convective boundary conditions. Advanced Powder Technology, 27(5), 2245–2256.

[3] Das SK, SUS Choi, Patel HE (2006) Heat transfer in nanofluids—a review. Heat Transf Eng 27(10):3–19.

[4] Yu W, France DM, Stephen US, Choi, Routbort JL (2007) Review and assessment of nanofluid technology for transportation and other applications. No. ANL/ESD/07–9. Argonne National Lab. (ANL), Argonne, IL (United States)

[5] Imtiaz, M., Hayat, T., & Alsaedi, A. (2016). Mixed convection flow of Casson nanofluid over a stretching cylinder with convective boundary conditions. Advanced Powder Technology, 27(5), 2245–2256

[6] Salahuddin, T., Malik, M. Y., Hussain, A., Awais, M., Khan, I., & Khan, M. (2017). Analysis of tangent hyperbolic nanofluid impinging on a stretching cylinder near the stagnation point. Results in physics, 7, 426-434.

[7] M. M. Bhatti and M. M. Rashidi, "Effects of thermo-diffusion and thermal radiation on Williamson Nano-fluid over a porous shrinking/stretching sheet," J. Mol. Liq., vol. 221, pp. 567–573, 2016.

[8] Ashorynejad HR, Sheikholeslami M, Pop I, Ganji DD. Nanofluid flow and heat transfer due to a stretching cylinder in the presence of magnetic field. Heat and Mass Transfer. 2013 Mar 1;49(3):427-36.

[9] Makinde, O.D. (2013) Effects of Viscous Dissipation and Newtonian Heating on Boundary-Layer Flow of Nanofluids over a Flat Plate. International Journal of Numerical Methods for Heat & Fluid Flow , 23, 1291-1303.

[10] Gorla, R. S. R., Chamkha, A. J., & Al-Meshaiei, E. (2012). Melting heat transfer in a nanofluid boundary layer on a stretching circular cylinder. Journal of Naval Architecture and Marine Engineering, 9(1), 1-10.

[11] Kasaeian, A., Daneshazarian, R., Mahian, O., Kolsi, L., Chamkha, A. J., Wongwises, S., & Pop, I. (2017). Nanofluid flow and heat transfer in porous media: a review of the latest developments. International Journal of Heat and Mass Transfer, 107, 778-791.

[12] Rana, P., & Bhargava, R. (2012). Flow and heat transfer of a nanofluid over a nonlinearly stretching sheet: a numerical study. Communications in Nonlinear Science and Numerical Simulation, 17(1), 212-226.

[13] Khan, W. A., & Pop, I. (2010). Boundary-layer flow of a nanofluid past a stretching sheet. International journal of heat and mass transfer, 53(11-12), 2477-2483.

[14] Rashid, M., Hayat, T., & Alsaedi, A. (2019). Entropy generation in Darcy–Forchheimer flow of nanofluid with five nanoarticles due to stretching cylinder. Applied Nanoscience, 9(8), 1649-1659.

[15] Pandey, A. K., & Kumar, M. (2017). Natural convection and thermal radiation influence on nanofluid flow over a stretching cylinder in a porous medium with viscous dissipation. Alexandria Engineering Journal, 56(1), 55-62.

[16] Sheikholeslami, M., Gorji-Bandpy, M., Ganji, D. D., Soleimani, S., & Seyyedi, S. M. (2012). Natural convection of nanofluids in an enclosure between a circular and a sinusoidal cylinder in the presence of magnetic field. International Communications in Heat and Mass Transfer, 39(9), 1435-1443.

[17] Ali Lund, L., Omar, Z., Khan, I., Raza, J., Bakouri, M., & Tlili, I. (2019). Stability analysis of Darcy-Forchheimer flow of Casson type nanofluid over an exponential sheet: Investigation of critical points. Symmetry, 11(3), 412.

[18] Ramachandra Prasad, V., Subba Rao, A., & Anwar Bég, O. (2013). Flow and heat transfer of casson fluid from a horizontal circular cylinder with partial slip in non-darcy porous medium. J Appl Computat Math, 2(2).

[19] Seth, G. S., Tripathi, R., & Mishra, M. K. (2017). Hydromagnetic thin film flow of Casson fluid in non-Darcy porous medium with Joule dissipation and Navier's partial slip. Applied Mathematics and Mechanics, 38(11), 1613-1626.

[20] Sheikholeslami, M. (2017). Influence of Lorentz forces on nanofluid flow in a porous cylinder considering Darcy model. Journal of Molecular Liquids, 225, 903-912.

[21] Hatami, M., & Ganji, D. D. (2013). Heat transfer and flow analysis for SA-TiO2 non-Newtonian nanofluid passing through the porous media between two coaxial cylinders. Journal of Molecular Liquids, 188, 155-161.

[22] Zeeshan, A., Maskeen, M. M., & Mehmood, O. U. (2018). Hydromagnetic nanofluid flow past a stretching cylinder embedded in non-Darcian Forchheimer porous media. Neural Computing and Applications, 30(11), 3479-3489.

[23] Dhanai, R., Rana, P., & Kumar, L. (2016). MHD mixed convection nanofluid flow and heat transfer over an inclined cylinder due to velocity and thermal slip effects: Buongiorno's model. Powder Technology, 288, 140-150.

[24] Hayat, T., Ijaz, M., Qayyum, S., Ayub, M., & Alsaedi, A. (2018). Mixed convective stagnation point flow of nanofluid with Darcy-Fochheimer relation and partial slip. Results in Physics, 9, 771-778.

[25] Muhammad, T., Alsaedi, A., Hayat, T., & Shehzad, S. A. (2017). A revised model for Darcy-Forchheimer three-dimensional flow of nanofluid subject to convective boundary condition. Results in physics, 7, 2791-2797.

[26] Sheikholeslami, M., & Bhatti, M. M. (2017). Forced convection of nanofluid in presence of constant magnetic field considering shape effects of nanoparticles. International Journal of Heat and Mass Transfer, 111, 1039-1049.

[27] Khan, M., Irfan, M., & Khan, W. A. (2018). Impact of heat source/sink on radiative heat transfer to Maxwell nanofluid subject to revised mass flux condition. Results in Physics, 9, 851-857.

[28] Waqas, M., Naz, S., Hayat, T., & Alsaedi, A. (2019). Numerical simulation for activation energy impact in Darcy–Forchheimer nanofluid flow by impermeable cylinder with thermal radiation. Applied Nanoscience, 9(5), 1173-1182.

[29] Chen, H., Liang, H., Xiao, T., Du, H., & Shen, M. (2016). Unsteady flow over an expanding cylinder in a nanofluid containing gyrotactic microorganisms. Canadian Journal of Physics, 94(5), 466-473.

[30] Haddad, Z., Abu-Nada, E., Oztop, H. F., & Mataoui, A. (2012). Natural convection in nanofluids: are the thermophoresis and Brownian motion effects significant in nanofluid heat transfer enhancement?. International Journal of Thermal Sciences, 57, 152-162.

[31] Xu, H., & Pop, I. (2014). Fully developed mixed convection flow in a horizontal channel filled by a nanofluid containing both nanoparticles and gyrotactic microorganisms. European Journal of Mechanics-B/Fluids, 46, 37-45.

[32] Xu, H., & Pop, I. (2014). Fully developed mixed convection flow in a horizontal channel filled by a nanofluid containing both nanoparticles and gyrotactic microorganisms. European Journal of Mechanics-B/Fluids, 46, 37-45.

[33] Chen, H., Liang, H., Xiao, T., Du, H., & Shen, M. (2016). Unsteady flow over an expanding cylinder in a nanofluid containing gyrotactic microorganisms. Canadian Journal of Physics, 94(5), 466-473.

[34] Fereidoon, A., Saedodin, S., Hemmat Esfe, M., & Noroozi, M. J. (2013). Evaluation of mixed convection in inclined square lid-driven cavity filled with Al2O3/water nano-fluid. Engineering Applications of Computational Fluid Mechanics, 7(1), 55-65.

[35] Chen, H., Liang, H., Xiao, T., Du, H., & Shen, M. (2016). Unsteady flow over an expanding cylinder in a nanofluid containing gyrotactic microorganisms. Canadian Journal of Physics, 94(5), 466-473.

[36] Ferdows, M., Reddy, M. G., Alzahrani, F., & Sun, S. (2019). Heat and mass transfer in a viscous nanofluid containing a gyrotactic micro-organism over a stretching cylinder. Symmetry, 11(9), 1131.

[37] Kuznetsov, A. V. (2010). The onset of nanofluid bioconvection in a suspension containing both nanoparticles and gyrotactic microorganisms. International Communications in Heat and Mass Transfer, 37(10), 1421-1425.

[38] Xu, H., & Pop, I. (2014). Mixed convection flow of a nanofluid over a stretching surface with uniform free stream in the presence of both nanoparticles and gyrotactic microorganisms. International Journal of Heat and Mass Transfer, 75, 610-623.

[39] Ishak, A., Nazar, R., & Pop, I. (2008). Magnetohydrodynamic (MHD) flow and heat transfer due to a stretching cylinder. Energy Conversion and Management, 49(11), 3265-3269.

[40] Sheikholeslami, M., & Rokni, H. B. (2017). Effect of melting heat transfer on nanofluid flow in existence of magnetic field considering Buongiorno Model. Chinese journal of physics, 55(4), 1115-1126.

[41] Rieger, H., & Beer, H. (1986). The melting process of ice inside a horizontal cylinder: effects of density anomaly.

[42] Khan, M., & Alshomrani, A. S. (2017). Characteristics of melting heat transfer during flow of Carreau fluid induced by a stretching cylinder. The European Physical Journal E, 40(1), 1-9.

[43] Bathelt, A. G., & Viskanta, R. (1980). Heat transfer at the solid-liquid interface during melting from a horizontal cylinder. International Journal of Heat and Mass Transfer, 23(11), 1493-1503.

[44] Hayat, T., Shah, F., Khan, M. I., & Alsaedi, A. (2017). Framing the performance of heat absorption/generation and thermal radiation in chemically reactive Darcy-Forchheimer flow. Results in Physics, 7, 3390-3395.

asma

ORIGINALITY REPORT

1%	1%	1%	1%
SIMILARITY INDEX	INTERNET SOURCES	PUBLICATIONS	STUDENT PAPERS

PRIMARY SOURCES

1	Submitted to Higher Education Commission Pakistan Student Paper	1%

Exclude quotes	On	Exclude matches	< 5 words
Exclude bibliography	On		

asma

GRADEMARK REPORT

FINAL GRADE

/10

GENERAL COMMENTS

Instructor

PAGE 1

PAGE 2

PAGE 3

PAGE 4

PAGE 5

PAGE 6

PAGE 7

PAGE 8

PAGE 9

PAGE 10

PAGE 11

PAGE 12

PAGE 13

PAGE 14

PAGE 15

PAGE 16

PAGE 17

PAGE 18

PAGE 19

PAGE 20

PAGE 21

PAGE 22

PAGE 23

PAGE 24

PAGE 25

PAGE 26

PAGE 27

PAGE 28

PAGE 29

PAGE 30

PAGE 31

PAGE 32

PAGE 33

PAGE 34

PAGE 35

PAGE 36

PAGE 37

PAGE 38

PAGE 39

PAGE 40

PAGE 41

PAGE 42

PAGE 43

PAGE 44

PAGE 45

PAGE 46

PAGE 47

PAGE 48

PAGE 49

PAGE 50

PAGE 51

PAGE 52

PAGE 53

PAGE 54

PAGE 55

PAGE 56

PAGE 57

PAGE 58

PAGE 59

PAGE 60

PAGE 61

PAGE 62

PAGE 63

PAGE 64

PAGE 65

PAGE 66

PAGE 67

PAGE 68

PAGE 69

PAGE 70